

AD-A173 397

CONSTITUTIVE EQUATIONS FOR DAMAGED CREEPING MATERIALS  
(U) MASSACHUSETTS INST OF TECH CAMBRIDGE DEPT OF  
MECHANICAL ENGINEERING G J RODIN AUG 86

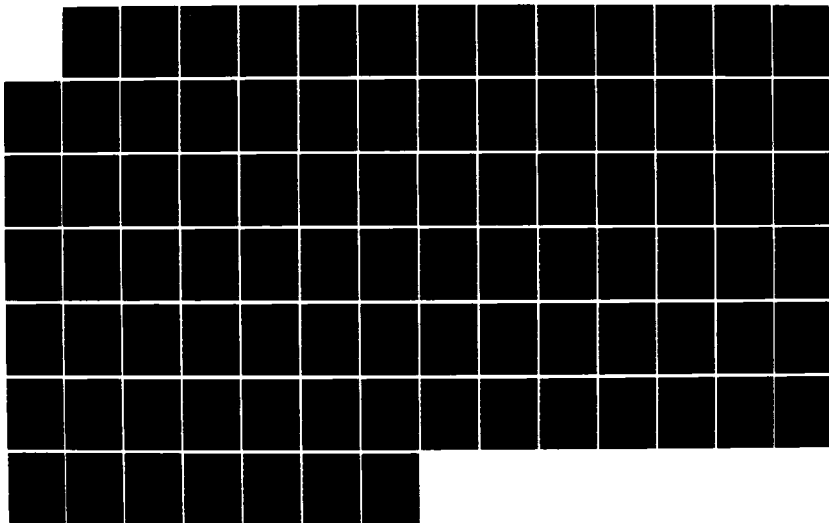
1/1

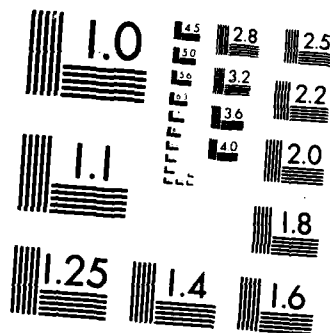
UNCLASSIFIED

N00014-80-C-0706

F/G 20/11

NL

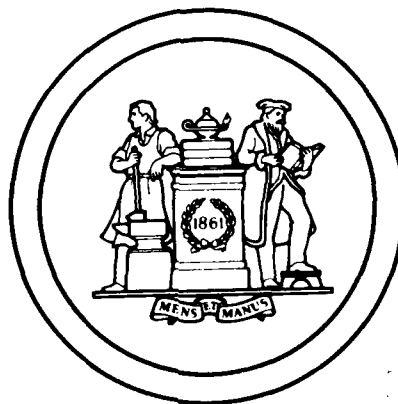
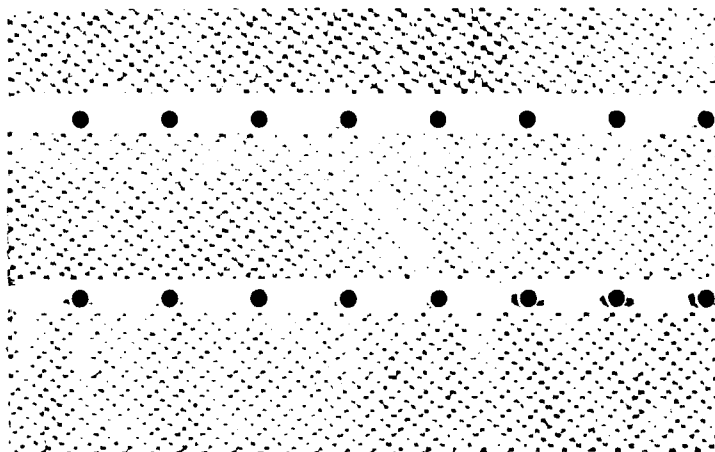




MICROCOPY RESOLUTION TEST CHART  
NATIONAL BUREAU OF STANDARDS-1963-A

**Reports of Research in  
Mechanics of Materials**

AD-A173 397



OCT 23 1986

A

OTIC FILE COPY

**Department of Mechanical Engineering  
Massachusetts Institute of Technology  
Cambridge, MA 02139**

86 9 15 211

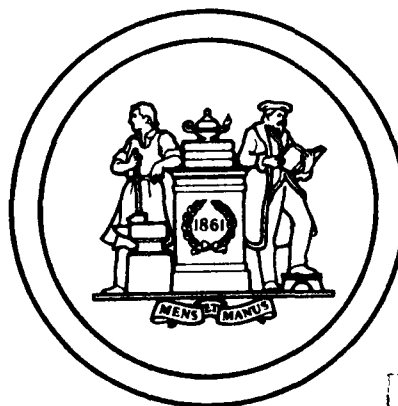
# Reports of Research in Mechanics of Materials

AD-A173 397

## CONSTITUTIVE EQUATIONS FOR DAMAGED CREEPING MATERIALS<sup>+</sup>

by

Gregory J. Rodin



OCT 23 1986

This document has been approved  
for public release and sale; its  
distribution is unlimited.

Department of Mechanical Engineering  
Massachusetts Institute of Technology  
Cambridge, MA 02139

OTIC FILE COPY

86 9 15 211

CONSTITUTIVE EQUATIONS FOR  
DAMAGED CREEPING MATERIALS†

by

Gregory J. Rodin

August, 1986

†This work was supported by ONR Solid Mechanics under grant N00014-80-C-0706.

# Constitutive Equations for Damaged Creeping Materials

by

Gregory J. Rodin

## Abstract

Constitutive equations for a power-law incompressible isotropic matrix containing aligned facet cracks are presented. Applications are directed to a description of polycrystalline materials which undergo significant tertiary creep when subjected to load at elevated temperatures. The main goal of the work is to develop three-dimensional constitutive relations for this class of materials and microstructural damage, which are both physically sound and straightforward to implement into a finite element program. Certain important features of the structure for such relations are emphasized. Some numerical and closed form solutions are presented to quantify the equations within the framework of the differential self-consistent scheme.



44

# Contents

<b>Preface</b>	<b>4</b>
<b>1 Introduction</b>	<b>8</b>
1.1 The Tensile Creep Curve . . . . .	8
1.2 Microscopic Observations . . . . .	11
<b>2 Applications of Continuum Mechanics</b>	<b>18</b>
2.1 Background . . . . .	18
2.2 Tensorial Representation . . . . .	24
2.3 Additional Remarks . . . . .	30
<b>3 Models of Damage</b>	<b>34</b>
3.1 Qualitative Features . . . . .	34
3.2 Quantification via the Differential Self-Consistent Scheme . . . . .	44
3.2.1 Background . . . . .	44
3.2.2 Numerical Analysis . . . . .	48
3.2.3 Linearized Solution . . . . .	52

3.2.4 Comparison of the Analyses. . . . .	55
4 Discussion	63
A Differentiation of the Eigenvalues with Respect to a Tensor.	79



# Chapter

## Preface

The demands of the nuclear, aerospace and other industries often subject engineering materials to extreme conditions of mechanical loads and elevated temperatures. Under these conditions, fracture is often a limiting performance criterion; therefore explicit consideration of the phenomenon is vital.

For temperatures above one-third of the absolute melting temperature, polycrystalline solids may undergo time dependent irreversible deformation: *creep*. The process is thermally activated and can lead to an eventual *creep fracture*.

A complete consideration of the problem requires an understanding of events ranging from local chemical reactions on an atomistic level to the formation of a macrocrack, which is easily visible. Contributions of such disciplines as physics, chemistry, materials science and mechanics have made possible significant progress towards important results; nevertheless the existing interdisciplinary gap still constitutes a major obstacle to interpretation of major aspects of creep. Therefore efforts directed at conceptual unification of our knowledge in the field should be a

worthwhile step to undertake.

There have been significant developments in metallurgical descriptions of mechanisms of deformation and fracture. Relations of these mechanisms to external factors such as level of applied stress and temperature, aggressiveness of environment, irradiation effects and many others are very important in engineering practice. A body of modeling efforts has been dominated by simplified mechanistic approaches (Ashby and Dyson, 1984), neglecting the crucial role of stress redistributions in inherently inhomogeneous polycrystals. On the other hand, the seminal idea of Kachanov (1958), broadly extended by subsequent research, resulted in large scale applications of *continuum damage mechanics*. The underlying internal variable structure of equations, which is very tractable for algorithmic treatment, fairly often presented materials in a black-box manner by neglecting metallurgical details of microstructural behavior.

A merger of these two approaches may produce fruitful grounds for constitutive formulations which include essential details of micromechanical behavior and the mathematical rigor of continuum mechanics. As an initial point we confine our attention to a derivation of macroscopic stress-strain relations for a mechanism commonly encountered in engineering and design practice – *intergranular creep fracture*. A set of parameters entering the description must, in principle, be extracted from limited microscopic or/and macroscopic measurements and have at least implicit

physical interpretations.

In the introduction we give both an overview of the traditional phenomenological approach and some observations on metallurgical processes which contribute to creep deformation and fracture. Relations between microscopically observed phenomena and externally applied stresses and temperature are crucial for further developments. The second chapter discusses a particular class of constitutive equations. The class generalizes major existing isotropic formulations, and can be applied to a very broad class of damage mechanisms. In the third chapter, we identify damage with a population of dispersed facet cracks. Quantification of equations is performed within the differential self-consistent scheme in a finite element environment. An alternative analytical procedure, employing linearization, presents a compact explicit expression which accurately follows the numerical results. The last part of the document summarizes the work and proposes directions for further research.

Finally, it is my great pleasure and privilege to acknowledge the care and support of those who contributed to this work.

I want to express my deepest admiration to David M. Parks for bearing with me for five years. If he had fun, then it was definitely mutual. I thank Professors Argon and Hutchinson for the enlightening experience of our short, but fruitful conversations.

I am infinitely indebted to Mary Toscano. She is the boss.

The help of my colleagues, especially Mary Boyce, Stuart Brown and Jim Papadopoulos is greatly appreciated.

I am grateful to DATA GENERAL CORPORATION for their major donation of the MV-10000 computer. The finite element computer program, ABAQUS, was made possible by HIBBITT, KARLSSON and SORENSEN, INC. through an academic license with the Massachusetts Institute of Technology.

This project was generously sponsored by the Office of Naval Research/Solid Mechanics under grant #N00014-80-C-0706. In particular, we express our gratitude to Dr. Alan Kushner.

Gregory Jacob Rodin

Cambridge, Massachusetts

August, 1986

# Chapter 1

## Introduction

### 1.1 The Tensile Creep Curve

The most conventional way of registering experimental data for creep deformation is the *creep curve* – a dependence of strain upon time under constant applied tensile load and temperature. Constant stress experiments are more valuable for identification of material response, but are also more difficult to conduct. At low creep ductilities, the difference may not be that important, and one can consider these experiments as interchangeable. Conversely, one should exercise care in interpreting data for higher creep ductilities. If creep strains are above ten percent, necking may substantially influence deformation (Ashby and Dyson, 1984). A schematic creep curve is shown in *Figure 1.1* We identify instantaneous elastic strain, followed by primary and tertiary stages. Within the present context, we view the secondary stage as the inflection point or the *minimum creep rate*.

Usually, more general relations of strain to time, temperature and stress are desired. A large number of empirical one-dimensional equations have been suggested

in attempts to quantify the phenomenon. Some important results in this direction were reviewed by Evans (1984). Forms reflecting a thermally activated nature of processes are widely accepted (Bird et al., 1969). The simplest relation between the minimum creep rate, temperature, and applied stress is

$$\dot{\epsilon}_{min} = \dot{\epsilon}'_0 \exp\left(-\frac{Q}{RT}\right) \left(\frac{\sigma}{\sigma_0}\right)^n = \dot{\epsilon}_0 \left(\frac{\sigma}{\sigma_0}\right)^n. \quad (1.1)$$

In the above equation,  $\dot{\epsilon}'_0$  and  $\sigma_0$  are the minimum athermal creep rate and the plastic deformation resistance at room temperature, respectively (Brown and Ashby, 1980). The activation energy,  $Q$ , and material exponent  $n$  are taken to be temperature independent, which is a sensible assumption for a wide range of practical situations (Evans, 1984);  $R$  is the universal gas constant. The importance of expression (1.1) lies in the possibility of its implication for both primary and tertiary stages. We associate the evolving plastic resistance with metallurgical processes accompanying the primary stage (Nix and Gibeling, 1985, Argon and Bhattacharya, 1986). The accelerating reference strain rate,  $\dot{\epsilon}'_0$ , conventionally reflects accumulation of damage, which is typical for the tertiary creep.

An extensive creep deformation may lead to creep fracture. In the absence of aggressive environments, fracture usually has intrinsic character, although for high stresses geometrical failure in the form of necking or rupture is possible. The fracture point is marked on the curve as  $t_f$  and  $\epsilon_f$ , on the horizontal and vertical axes, respectively. Both time to fracture and strain to fracture are important parameters

in design considerations. Monkman and Grant (1956) proposed a very valuable empirical expression to relate the time to fracture to the minimum creep rate

$$\dot{\epsilon}_{min}^{\beta} t_f = C. \quad (1.2)$$

Both constants  $\beta$  and  $C$  exhibit remarkable independence from temperature for a wide range of temperatures and materials (Evans, 1984). Exponent  $\beta$  typically varies from .7 to 1.; these bounds correspond to transition from intrinsic fracture to geometric failure. Constant  $C$  is usually about .01 (sec)<sup>1- $\beta$</sup> .

These two equations are the most accepted formulas of phenomenological approaches. They present an important tool for design considerations and may be sufficient for a limited class of practical situations. Complexity increases substantially in the presence of multiaxial non-stationary stressing and temperature histories, where current understanding is far from satisfactory. Part of the failure to obtain a reasonably unique recipe is a direct consequence of drastic oversimplification of the diversity of creep deformation and fracture. On the other hand, an attempt to treat creep on finer scales, for example metallurgical, may be an impossible task, in terms of structural applications and design. In this work we seek a partial resolution through a combination of the most basic phenomenological and metallurgical facts.

## 1.2 Microscopic Observations

The objective of this section is to give *necessary* information about microscopic aspects of creep. Review of research in this field is an honorable task, and it has been very successfully accomplished by Argon (1982), Ashby, et al. (1979), Cocks and Ashby (1983), Frost and Ashby (1982), Nix and Gibeling (1985) and others. The book by Evans (1984) is my favorite source, and though some ideas expressed there may be too subjective, this subjectivity contributes to the book's value.

A representation of deformation and fracture for a given metal or alloy may be given in terms of identification of possible mechanisms and conditions for a dominance of individual mechanism(s) over the others – the *fracture map* (Ashby, et al., 1979). The fracture map for Nimonic 80A is shown on *Figure 1.2*. On the horizontal axis we measure time in seconds and on the vertical axis a tensile stress normalized by the Young's modulus. For different external conditions one can identify the dominant mechanism of fracture. For a practical range of temperatures and stresses, *intergranular creep fracture* is important. This map is very typical for a broad class of metals and alloys, and therefore our further attention is confined to behavior related to intergranular fracture. Information one may extract from a fracture map is the termination diagnosis, and is not sufficient to reproduce the whole history. Nevertheless, the mechanism of fracture indirectly predicts the nature of preceeding deformation within a context of microscopical processes. To us, the most philosoph-



ically appealing approach is to accept the situation as a single, though very diverse evolution, thus to avoid as much as possible conditional classifications. The complexity involved and an incomplete understanding of individual stages forces us to a level of studying separated phenomena on their particular scales without solid interrelations.

An alternative to phenomenological considerations of the previous section is a description of creep in terms of three related metallurgical processes: hardening, recovery and cavitation <sup>1</sup>. Hardening can be loosely associated with an increase in the dislocation density. Recovery is a converse process of annihilation of dislocations with opposite Burger's vectors. Cavitation is a continuous process of nucleation, growth and coalescence of voids. The first two processes are usually central to primary creep and they microscopically reflect the structure of dislocations. Some more recent results (Argon and Bhattacharya, 1986) suggest that the steady state of hardening and recovery may not correspond to the time of the minimum creep rate. This is in agreement with a proposition of Ashby and Dyson (1984) that tertiary creep may be substantially influenced by recovery. Obviously, a "complete" treatment would require consideration of these processes *per se* and their interrelations. This task probably stands far away from our current state of knowledge and abilities. In this work, we confine our attention to modeling of cavitation which precedes intergranular fracture.

---

<sup>1</sup>We do not explicitly mention aging, although it can be indirectly included into the description.

The initiation process of intergranular fracture is the nucleation of grain boundary voids. There is no definite assignment of a particular mechanism to this stage, though there are serious reasons to treat it as agglomeration of vacancies on stressed interfaces (Argon, et. al, 1980). Grant and Mullendore (1965), and Servi and Grant (1951) recognized the importance of the presence of two factors: grain boundary sliding, and hard second phase particles. Grain boundary sliding is a very important independent mechanism of deformation. It is sensibly localized shear deformation at a grain boundary which produces relative offsets of one grain with respect to another. In principle, grain boundary sliding induces incompatible strains, which must be accommodated by the surrounding matrix. Accomodation causes stress concentrations in the vicinity of the hard particles and triple point junctions. Some predictions (Argon, et. al, 1980) suggest that for typically applied stress of 10 MPa, nucleation stresses should be about 100 MPa. At present, it is still unclear how such high stress concentrations can be generated. The recently developed small angle neutron scattering technique allows for resolution up to  $10^{-8}m$ , which is not sufficient to directly observe the nucleation of voids, but enables us to see stable cavities with characteristic dimensions of  $\sim 10^{-7}m$  (Yang, et. al, 1983). A detailed review by Argon (1982) underlines thermodynamical basis of nucleation, thus providing an insightful approach to the subject.

The next natural step in cavities' evolution is their growth. There are three dis-

tinct mechanisms: grain boundary diffusion, surface diffusion and power-law creep of the surrounding matrix. A large collection of *deformation-mechanism maps* by Frost and Ashby (1982) reveals the practical importance of diffusion processes. Nevertheless, at higher stresses, the growth rate is controlled by a creeping matrix (Needleman and Rice, 1980). In principle, any combination of mechanisms is possible; dominance of one or another depends upon a variety of parameters. Continuous void nucleation and growth on a grain boundary lead to collapse of ligaments and eventual formation of a *facet crack*. Such crack has dimensions of a grain ( $\sim 10^{-5}m$ ) and is the most accessible microscopic entity for observations. Accumulation of damaged facets may cause the localized formation of a macroscopic crack, the fast propagation of which manifests the final failure. It is important to realize that the above schematic procedure describes local events within one grain boundary. In reality one may observe various stages on distinct grain boundaries, though individual processes are intimately related for neighboring grains.

In order to characterize damage accumulation we should answer three keystone questions:

- What is damage?
- How does it influence material behavior?
- How does it accumulate?

Phenomenological theories usually omit the first question. On the other hand, it

seems to be the most natural way to approach modeling. Our brief review suggests that a void is most basic entity throughout a cavitation process and therefore it should represent damage. On the other hand, we have to bear in mind that it is not a single void that the most important to us, but a population of a very large number of voids. It is inevitable in this situation to employ a statistical approach, in order to obtain some sensible interpretations. Therefore, we have to take into account both physical significance and probabilistic assessment of damage. Let us consider some qualitative features of the latter. We may probably claim a random distribution of hard particles both throughout a volume of a specimen and on grain boundaries (Argon, et al., 1984). This assumption allows us to claim that *spatial (of course not directional)* distribution of cavitated grain boundaries should be random within the specimen as a whole. Therefore, in terms of voids we have a superposition of statistics: on the global level – grain boundaries, on the local level – the individual structure of a boundary. It is obvious that even with simplified assumptions (i.e., of planar boundaries, of globally equivalent grain boundaries having identical local statistics, and others), treatment of intergranular fracture on a level of voids is extremely complicated. Moreover, any experimental program directed towards development of sufficient data must take tremendous effort and may not pay off in the end. It should be advantageous to do some preliminary “work” on the individual grain boundary and then incorporate it into

some global statistics. The above situation has a fairly clear interpretation in terms of scales. There are three distinct length dimensions: macro – specimen, mini – grain boundary and micro – void. If voids represent damage, then one should be able to draw a straight path to the macro scale. We propose some kind of decoupling – micro to mini and mini to macro. It should be a better assumption for more dilute cavitations, when we may claim that whatever is happening on one grain boundary is unrelated to events on the others.

In this work we concentrate on the second path and we like to employ the suggestion of Rice (1981) for a simple way to represent a grain boundary. The population of cavitated grain boundaries ranges from practically undamaged boundaries to fully developed facets. Response of a cavitated boundary strongly depends on a number of geometric physical parameters. In order to gain some simplicity in modeling, we represent the manifold of cavitated grain boundary by a penny-shaped crack with a distribution of uniform normal tractions applied to the flanks. Naturally, zero tractions correspond to a fully developed facet crack, while fully loaded flanks should model an uncavitated boundary. This idea has been further applied by Anderson and Rice (1984), and by Tvergaard (1985).

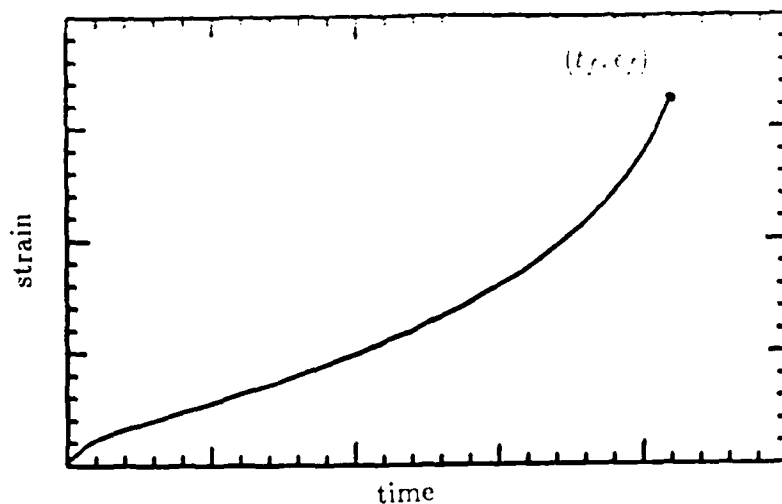


Figure 1.1 A Schematic Creep Curve

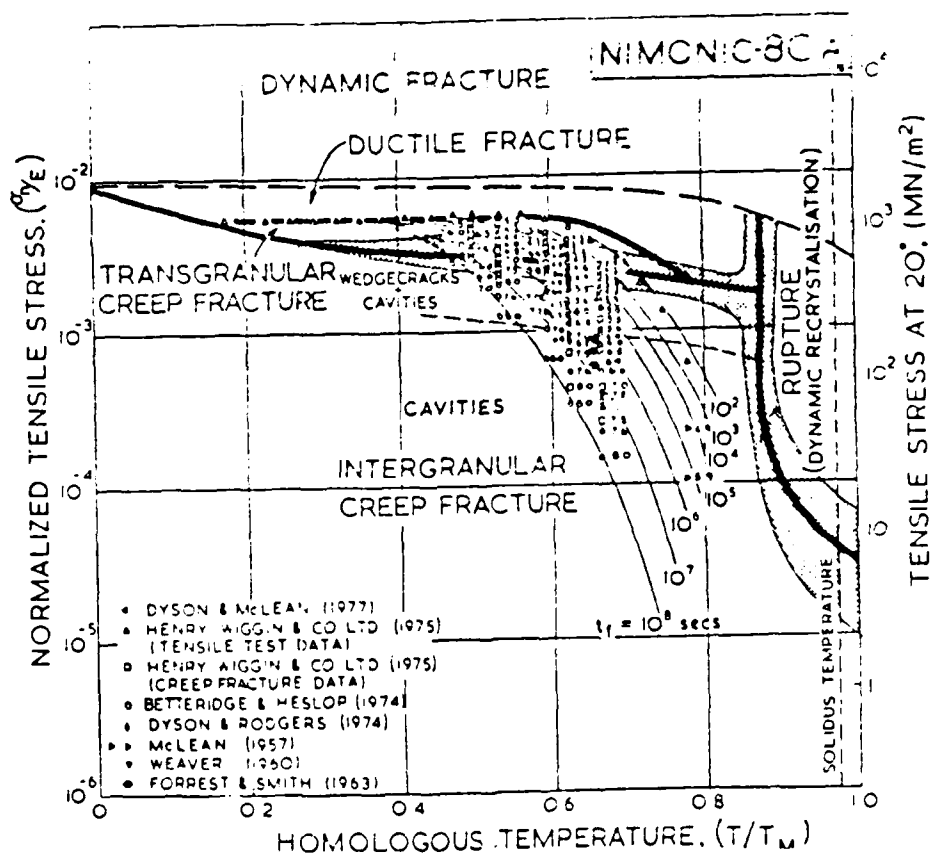


Figure 1.2 Fracture Map (From Ashby et al., 1979)

## Chapter 2

# Applications of Continuum Mechanics

### 2.1 Background

Prior observations on metallurgical and mechanical response at elevated temperatures strongly suggest the adoption of a state variable framework for formulating a set of constitutive equations. A consistent approach requires identification of:

- state variables
- constitutive stress-state-strain rate relations
- evolutionary equations
- initial and terminal conditions.

In the case of creep deformation and fracture, we assert that the state variables should be associated with the distribution of dislocations and degree of cavitation, or simply damage. Let us designate the first group of such internal variables by  $\lambda$ ,

and the second group by  $\rho$ . Following Rice (1970), we write a set of the equations for isotropic isothermal response in a form

$$\mathbf{E} = \mathbf{E}^e + \mathbf{E}^c, \quad (2.1)$$

$$\mathbf{E}^e = \frac{1}{2G} \mathbf{T} + \frac{1-\nu}{6G(1+\nu)} (\text{tr} \mathbf{T}) \mathbf{I}, \quad (2.2)$$

$$\dot{\mathbf{E}}^c = \dot{\mathbf{E}}^c(\lambda, \rho, \mathbf{T}); \quad (2.3)$$

$$\dot{\lambda} = \dot{\lambda}(\lambda, \rho, \mathbf{T}); \quad (2.4)$$

$$\dot{\rho} = \dot{\rho}(\lambda, \rho, \mathbf{T}); \quad (2.5)$$

$$\mathbf{E}^c = \mathbf{E}_0^c, \quad \lambda = \lambda_0, \quad \rho = \rho_0, \quad \text{at } t = 0; \quad (2.6)$$

$$H(\lambda, \rho) = 0, \quad \text{at } t = t_f. \quad (2.7)$$

In the above equations boldface  $\mathbf{T}$  and  $\mathbf{E}$  denote the stress and the strain tensors, respectively;  $\mathbf{I}$  is the second rank identity tensor in three-dimensional space. The superscripts correspond to elastic and creep components. Elastic material response is characterized by the shear modulus  $G$  and the Poisson's ratio  $\nu$ . If we view stresses as an input, than we can solve evolutionary equations (2.4),(2.5) with the initial conditions (2.6) for  $\lambda$  and  $\rho$ . Termination condition (2.7) implicitly defines  $t_f$ , the time to fracture. Finally, creep strain rate-state-stress equation (2.3) should be integrated in order to complete the system.



The pioneering step in using this framework was undertaken by Kachanov (1958) by introducing a one-dimensional model with one internal variable – continuity, equal to one for an undamaged material and equal to zero at fracture. Rabotnov (1960) extended the result and introduced a complementary variable – damage,  $\omega$ . The later developments of Leckie and Hayhurst (1974), currently the most accepted damage formalism, provided three-dimensional constitutive and evolution equations. The creep strain rate-state-stress relations were taken in the form similar to Norton's law. The evolutionary equation for  $\omega$  was dependent upon a linear combination of the Mises stress, the maximum principal tensile stress, and the hydrostatic pressure. The subsequent papers of Leckie and Hayhurst (1977), Hayhurst and Leckie (1983), Hayhurst (1983), Hayhurst et al., (1983) contributed to the identification of material constants, further refinements and analyses of some basic configurations. A detailed investigation of Riedel (1984) concentrated on crack tip behavior in damaging material. Possible extensions of the damage mechanics of Kachanov, Rabotnov, Leckie and Hayhurst are proposed by Murakami (1983), Onat (1982), Onat and Leckie (1984) and Krajcinovic (1983). These studies include treatments of anisotropic finite deformation, employment of tensorial damage state and thermodynamical restrictions. These developments, although very far from being complete, have significantly improved analytical abilities in the field, but nevertheless it is fair to say that only intuitive, semi-naïve parallels to the microscale have

been drawn thus far.

A complete formulation of system (2.1)-(2.7) is beyond the scope of our present goals, and we shall concentrate on equation (2.3). We freeze internal structure and seek the instantaneous response of material. This mathematically natural, but physically problematical situation (how to conduct and control such a test?) is a fundamental starting point (Nix and Gibeling, 1985).

We identify set  $\lambda$  with the dislocation density. According to Taylor's rule (Nix and Gibeling, 1985), the deformation resistance is

$$\sigma_0 = 3Gb\sqrt{\lambda}, \quad (2.8)$$

where  $b$  is the length of the Burger's vector.

The damage set  $\rho$  must implicitly quantify the population of cavitated grain boundaries. Let us consider a volume,  $V$ , occupied by  $N$  equal planar penny-shaped cracks of radius  $a$ . Crack face tractions are not taken into account until the last chapter, where we note a very tractable alternative for including them into the equations. One conceptual possibility of analysis can be associated with the classical continuum mechanics. Unfortunately, the boundary-value problems arising from this formulation are characterized by extremely complicated geometries, and we are unable to obtain complete solutions. On the other hand, very important qualitative features of these solutions will be presented in the next chapter.

We address mechanics of a continuum with microstructure (Kunin, 1982, 1983) as a major insightful alternative. Every crack is completely prescribed by three coordinates of the center and two orientation angles of the normal to the plane. The radius is common for all the cracks, therefore; there are  $5N + 1$  pieces of information to describe this particular damage. A sufficiently large number of cracks should provide ideal ground for a statistical approach, but we may equally enjoy a much simpler view. Namely, for the given volume and the crack radius, the state of damage is to zeroth order characterized by the number of cracks *per se*. The single, dimensionally appropriate parameter, the crack density, is (Budiansky and O'Connell, 1976)

$$\rho := \frac{a^3 N}{V}. \quad (2.9)$$

We observe that the square root of the dislocation density, multiplied by the magnitude of the Burger's vector, may be understood as a similar reduction for a population of dislocations. Therefore, we can argue some consistency for our choice of the parameters.

Equations (2.1)-(2.7) are written for a material point; thus, we should be concerned with a careful explanation of the meaning of the crack and the dislocation densities at the latter. We may follow a usual routine for these concepts. We choose a sphere <sup>1</sup> inside the body. The center is at point  $\mathcal{P}$ , and the radius of the sphere

---

<sup>1</sup>The choice of a sphere is not essential. It allows us to keep the presentation simple. In the third chapter, where we encounter boundary-value problems, we prefer a circular cylinder.

is  $r$ . We can formally establish the crack density for the sphere via (2.9). It would be natural to suggest that the value of  $\rho$  *at the point* is the appropriate limit as the radius of the sphere tends to zero. We are interested in locating a sufficient number of cracks *inside* the material point, rather than in the number of cracks *per se*. If there are few cracks within the large sphere, then we attribute the case to a dilute population. Therefore, the finiteness of the cracks' size imposes additional restrictions on the definition of the crack density at a point. The compromise: we choose the radius of the sphere to be large relative to the cracks' radius, and small compared to characteristic dimensions of the body to which continuum mechanics is to be applied. Again, large and small are purely judicious terms, and we avoid any speculations here. The same logic is applicable for the dislocation density.

A procedure for reducing problems with two or more characteristic length scales to classical continuum formulations is termed *homogenization*. To some extent, we smear or homogenize the actual distributions of the cracks by presenting them via the field or continuous variable. The dependence of material response upon the crack density is the major technical effort of this research. We split the problem into two parts. The first part is related to the influence of the population of cracks on the tensorial aspects of the constitutive equation (2.3). The next chapter completes the problem by presenting an alternative method of quantifying tensorial forms which arise.

## 2.2 Tensorial Representation

Within the context of Norton's law, relations (2.3) for the infinitesimal creep strain rates are adopted. Undamaged matrix creep response is taken to be incompressible isotropic governed by a strain rate potential <sup>2</sup>

$$F = \frac{\sigma_0 \dot{\epsilon}_0}{n+1} \left( \frac{\bar{\sigma}}{\sigma_0} \right)^{n+1}, \quad (2.10)$$

where the Mises equivalent stress is

$$\bar{\sigma} = \left( \frac{3}{2} \mathbf{S} \cdot \mathbf{S} \right)^{\frac{1}{2}}, \quad (2.11)$$

and the stress deviator is

$$\mathbf{S} = \mathbf{T} - \frac{1}{3} (\text{tr} \mathbf{T}) \mathbf{I}. \quad (2.12)$$

The traceless strain rate tensor  $\dot{\mathbf{E}}^c$  is derived from (2.10), as a gradient in the  $\mathbf{T}$ -space. There are three important features of the dependence of the strain rate potential on stress to be emphasized:

- it is a function of one scalar variable
- it is a homogeneous function of  $\mathbf{T}$  of degree  $n+1$
- it is convex in  $\mathbf{T}$ -space.

---

<sup>2</sup>This section heavily employs material of the paper by Rodin, G.J., Parks, D.M., (1986) 'Constitutive Models of a Power-Law Matrix Containing Aligned Penny-Shaped Cracks,' to be published in 'Mechanics of Materials'.

The first two statements are transparent; the last statement can be verified by showing that  $\bar{\sigma}$  satisfies Schwartz's inequality in  $\mathbf{T}$  (Vainberg, 1964). We assume that the last two properties are preserved for a macro response of the matrix with cracks.

It is obvious that for an arbitrary distribution of cracks, material generally loses its initial isotropy and the number of variables in the description of the problem increases drastically. Experimental observations (Johnson et al., 1962, Trampczynsky et al., 1981) suggest that the majority of cracks are found on the grain boundaries normal to the direction of the maximum principal applied macroscopic tensile stress  $\sigma_1$ . Therefore, the assumption that the aligned cracks are otherwise randomly located allows us to postulate a transversely isotropic macro response.

There is a large class of situations of substantial practical interest, where engineering structures are subjected to proportional load histories. As long as the proportional loading does not alter the direction of the principal stress in time, the cracks are locally oriented in a direction which is unrelated to any preferred material orientation. The above is nothing but a definition of an isotropic material. This conclusion was drawn by Hutchinson (1983) and Duva and Hutchinson (1983) to derive constitutive relations for dilute concentrations of aligned cracks.

The idea is quite compatible with the phenomenological damage mechanics (Leckie and Hayhurst, 1974), where isotropy is assumed and a representative stress

$$\bar{\sigma} = \alpha_1 \bar{\sigma} + \alpha_2 \sigma_1 + \frac{\alpha_3}{3} \text{tr} \mathbf{T}, \quad \sum_{k=1}^3 \alpha_k = 1, \quad (2.13)$$

implicitly enters into the constitutive relations via the evolution equation for a single damage parameter. For a wide class of metals the value of  $\alpha_3$  is small (Hayhurst and Leckie, 1983), and is set to zero in the analysis.

Within the framework of the above assumptions we claim that the material is characterized by a function  $\hat{F}$  which is both convex and homogeneous in stresses:

$$F = \hat{F}(\sigma_0, \dot{\epsilon}_0, n, \bar{\sigma}, \sigma_1, \rho). \quad (2.14)$$

It is important to bear in mind that at  $\rho = 0$ , expression (2.14) is identical to (2.10).

On dimensional grounds, we claim that the creep rate potential can be written:

$$F = \frac{\sigma_0 \dot{\epsilon}_0}{n+1} f(n, \rho, x) \left( \frac{\bar{\sigma}}{\sigma_0} \right)^{n+1}. \quad (2.15)$$

Expression (2.15) preserves the homogeneity of  $F$  by introduction of a new variable  $x$

$$x := \frac{\sigma_1}{\bar{\sigma}}. \quad (2.16)$$

The description of the material reduces to the construction of a scalar function  $f$  of three dimensionless variables. The first variable describes the matrix response, the second is the averaged characteristic of the microstructural topology, and  $x$  identifies the stress state. Convexity of the potential is guaranteed if a positive function  $f(n, \rho, x)$  of (2.15) satisfies (Rodin and Parks, 1986a)

$$ff'' - \frac{n}{n+1}f'^2 \geq 0, \quad (2.17)$$

where prime denotes differentiation with respect to  $x$ .

The tensorial quantities derivable from (2.15) by straightforward differentiation are the creep strain rate and the compliance tensors; they are written in terms of the derivatives of  $f$  with respect to  $x$  and the derivatives of the stress invariants with respect to the stress tensor itself. One of the motivations for this work is to derive an effective framework for solving boundary-value problems using the material model. As the vast majority of problems require numerical analysis, we have to comply with the requirements of a standard displacement-based finite element procedure. Therefore, it is necessary to invert both the strain rate/stress relations and the compliance tensor. Direct numerical inversion of the material point stiffness tensor within a finite element code can represent a significant computational cost, while conversely the algebraic expression of the stresses and the stiffnesses in terms of the strain rates can provide economies.

The sequence of steps leading to the algebraic forms includes the derivation of the strain rate/stress relations from (2.15), their inversion, and then differentiation with respect to the strain rate tensor.

The strain rates are given by (Appendix)

$$\dot{\mathbf{E}}^c := \frac{\partial F}{\partial \mathbf{T}} = \dot{\epsilon}_0 \left[ \frac{3}{2} \left( f - \frac{xf'}{n+1} \right) \frac{\mathbf{S}}{\bar{\sigma}} + \frac{f'}{n+1} \mathbf{e}_1 \otimes \mathbf{e}_1 \right] \left( \frac{\bar{\sigma}}{\sigma_0} \right)^n. \quad (2.18)$$



In the above formula  $\mathbf{e}_1$  is the unit eigenvector corresponding to the maximum principal stress. The tensorial quantities in (2.18) appear as the result of the differentiation of  $\bar{\sigma}$  and  $\sigma_1$  with respect to the stress tensor (Appendix).

The first term in the square brackets of (2.18) governs the deviatoric response of the material, and has structure similar to the incompressible matrix. The second term contributes to the volumetric expansion, and it disappears if there are no cracks. We assume that both scalar premultipliers are nonnegative. The first premultiplier is assumed nonnegative so that the macroscopic deviatoric power, like that of the underlying matrix, is nonnegative. If we take the trace in (2.18), then we note that the second premultiplier is the strain rate dilatation and, therefore, is nonnegative.

One of the features of isotropic constitutive equations of this class is the equivalence of the corresponding eigenvectors of the stress and the strain rate tensors. This fact allows us to reinterpret the vector  $\mathbf{e}_1$  in (2.18) as the maximum principal creep strain rate eigenvector.

Let us introduce the modified deviator of the strain rate tensor, given by

$$\mathbf{D} := \dot{\mathbf{E}}^c - (\text{tr} \dot{\mathbf{E}}^c) \mathbf{E}_{11}, \quad (2.19)$$

with the invariants

$$\bar{\kappa} := \left( \frac{2}{3} \mathbf{D} \cdot \mathbf{D} \right)^{\frac{1}{2}}, \quad \kappa_1 := \mathbf{D} \cdot \mathbf{E}_{11}. \quad (2.20)$$

Tensor  $\mathbf{E}_{11}$  belongs to the set of tensors defined as the dyadic products  $\mathbf{E}_{ij} := \mathbf{e}_i \otimes \mathbf{e}_j$ , where  $\mathbf{e}_i$  ( $i, j = 1, 3$ ) denote eigenvectors of  $\mathbf{T}$ . Simple algebra leads to the conclusion that the new invariant  $\bar{\kappa}$  is the partial derivative of the strain rate potential  $F$  with respect to the Mises stress  $\bar{\sigma}$ , which in turn establishes the dual pairs of invariants  $\bar{\sigma} \Longleftrightarrow \bar{\kappa}$ ,  $\sigma_1 \Longleftrightarrow \text{tr} \dot{\mathbf{E}}^c$ .

It was suggested by Rodin and Parks (1986a) that introduction of the function dual to  $x$  defined as

$$y := \frac{\text{tr} \dot{\mathbf{E}}^c}{\bar{\kappa}} = \frac{f'}{(n+1)f - xf'}, \quad (2.21)$$

is beneficial, because it enables us to rewrite the convexity condition (2.17) as the requirement for  $y(x)$  to be monotone increasing, and, therefore, sets up a one to one correspondence between  $x$  and  $y$  for positive  $x$  and recovers the incompressible response for  $x \leq 0$ .

An algorithmic procedure for the inversion and the stiffness fourth-rank tensor may be based on the Legendre transform. The key point is that we have established pairs of conjugate invariants  $\bar{\sigma} \Longleftrightarrow \bar{\kappa}$  and  $\sigma_1 \Longleftrightarrow \text{tr} \dot{\mathbf{E}}^c$ , which in turn allows us to define a dual stress potential

$$G := \bar{\sigma} \bar{\kappa} + \sigma_1 \text{tr} \dot{\mathbf{E}}^c - F = \frac{n}{n+1} \sigma_0 \dot{\epsilon}_0 \frac{(1 + yx(y))^{\frac{n+1}{n}}}{f(n, \rho, x(y))^{\frac{1}{n}}} \left( \frac{\bar{\kappa}}{\dot{\epsilon}_0} \right)^{\frac{n+1}{n}}. \quad (2.22)$$

We can express all entries related to the stress tensors in terms of the strain rate invariants and pursue the main point by stating

$$\mathbf{T} = \frac{\partial G}{\partial \dot{\mathbf{E}}^c}. \quad (2.23)$$

The second derivative of  $G$  with respect to the strain rate tensor, is the stiffness tensor. We do not give the expression for the latter, but it is given by Rodin and Parks (1986b).

## 2.3 Additional Remarks

In the previous section we derived tensorial forms characteristic for the class of constitutive equations which are governed by the maximum principal tensile stress and the Mises stress. The required differentiation of the eigenvalues with respect to their tensor was implicitly assumed to be a proper mathematical operation. This is not necessarily true in the case of repeated eigenvalues. A comprehensive treatment of the subject applied to second rank tensors in two- and three-dimensional Euclidean spaces was recently given by Carlson and Hoeger (1984).

Let us suppose that the principal stresses satisfy  $\sigma_1 = \sigma_2 > \sigma_3$ . In this case directions  $\mathbf{e}_1$  and  $\mathbf{e}_2$  can be *any* pair of orthogonal vectors lying in the plane perpendicular to the vector  $\mathbf{e}_3$ . Moreover, the derivative of  $\sigma_1$  with respect to the stress tensor does *not exist*. As  $\mathbf{e}_1$  appears in the constitutive equations (2.18) due to the differentiation, we conclude that our definitions should be refined.

The contradiction has a physical explanation. For the purpose of demonstration, we consider a set of  $2M + 1$  thin rectangular sheets, which are subjected to uniform

biaxial tension in the plane. This is a typical plane stress situation. We may associate distributed loads with the macroscopic principal stresses  $\sigma_1, \sigma_2, 0$ . All specimens are identical prior to load application and are formed from undamaged material. We fix load  $\sigma_1$ , and apply different  $\sigma_2$  for every specimen. The second load for the  $m^{\text{th}}$  specimen is

$$\sigma_2^m = \frac{m + M}{2M + 1} \sigma_1, \quad m = 1, 2, \dots, 2M + 1. \quad (2.24)$$

Obviously, for the first  $M$  specimens,  $\sigma_1$  is the maximum stress, the  $M + 1^{\text{st}}$  specimen is subjected to equal biaxial tension, and for the rest  $\sigma_2$  is the maximum stress. According to the adopted assumptions, the first subset of specimens should develop cracks in the direction normal to  $\sigma_1$ . Isotropy requires the  $M + 1^{\text{st}}$  specimen to have equibiaxial distribution of cracks, which logically coincides with experimental observations (Hayhurst, 1983). Naturally, the remaining subset develops cracks orthogonal to those in the first  $M$  specimens. For large  $M$  the ambiguity is obvious: an essentially continuous variation of the stress produces the discontinuity in the orientation of damage. If we take very large  $M$ , the stress states are very close, and the difference between the  $M^{\text{th}}$ ,  $M + 1^{\text{st}}$  and  $M + 2^{\text{nd}}$  specimens should be very small. However, we observe three distinct damage fields.

In order to avoid this conceptual gap, we must introduce a model which accounts for multiaxial stress state in a more general manner. For example, Chen and Argon (1981) suggested that in uniaxial tension, a  $\cos^2\theta$  distribution of cavitated grain

boundaries should occur. Angle  $\theta$  is measured between  $\mathbf{e}_1$  and the normal to a crack. Though this may be a more accurate statement than the one we have been using, it still does not handle repeated eigenvalues.

An alternative formal way to treat the singularity is to parametrically imbed the maximum principal stress into a sequence  $\sigma^{(p)}$ , which, in the infinite limit of the parameter,  $p$ , gives

$$\sigma_1 = \lim_{p \rightarrow \infty} \sigma^{(p)}. \quad (2.25)$$

A choice of a suitably large but finite  $p$  may provide both a good approximation and unique differentiation. A possible sequence is

$$\sigma^{(p)} := \frac{1}{p} \ln \left( \frac{\text{tr}(\exp(p\mathbf{T}))}{3} \right) = \frac{1}{p} \ln \left( \frac{\exp(p\sigma_1) + \exp(p\sigma_2) + \exp(p\sigma_3)}{3} \right) \quad (2.26)$$

It can be shown (Appendix) that equation (2.25) is satisfied and the above invariant can be differentiated for any value of the tensorial argument.

Another advantage of the introduced parametric invariant is that

$$\sigma^{(0)} = \lim_{p \rightarrow 0} \sigma^{(p)} = \frac{1}{3} \text{tr} \mathbf{T}, \quad (2.27)$$

which leaves room for some extensions to include voided power-law materials (Budiansky et al., 1981, Duva and Hutchinson, 1983, Duva, 1986). Some experimental observations (e.g. the review by Onat and Leckie, 1984) implicitly suggest that transgranular cavitation and hot ductile rupture may be described by the hydrostatic pressure, rather than the maximum principal stress, in addition to the Mises

stress. Therefore we may indirectly unify a formalism for both intergranular and transgranular mechanisms of fracture.

In general, there are obvious drawbacks related to the new invariant. Unfortunately  $\sigma^{(p)}$  is not a homogeneous function of the stress tensor, which prohibits representation (2.15) central for the work. We assume that a formal preservation of the latter by putting

$$x = \frac{\sigma^{(p)}}{\bar{\sigma}} \quad (2.28)$$

is acceptable, though we can not defend it with confidence. Another drawback accompanying this refinement is the absence of the algebraic Legendre transform, which instead must be done numerically and may possibly increase computational expense. It is obvious that in the case of  $p = 0$ , we do have all of the features described in the previous section, and a proper differentiation.

## Chapter 3

# Models of Damage

### 3.1 Qualitative Features

The previous chapter was centered on the derivation of the general tensorial form, which should be completed by specifying a scalar function of the three variables – material exponent,  $n$ , crack density,  $\rho$ , and triaxiality,  $x$ . Here we are interested in possible ways of constructing the function. First of all, we would like to relate our framework to the phenomenological damage mechanics. Fracture may be associated with some critical value of the crack density,  $\rho_f$ . The standard notation of the Kachanov-Rabotnov-Leckie-Hayhurst equations is generated by the two following equations:

$$\omega = \frac{\rho}{\rho_f}, \tag{3.1}$$

$$f(n, \rho, x) = \left( \frac{1}{1 - \omega} \right)^n = \left( \frac{\rho_f}{\rho_f - \rho} \right)^n. \tag{3.2}$$

We expect the above given function to predict an

incompressible response. Substitution of (3.2) into constitutive equations (2.18) reveals that, formally, incompressibility is equivalent to  $f'(n, \rho, x) = 0$ . We also conclude that the critical crack density must be independent of the triaxiality. The phenomenological nature of equations (3.1),(3.2) is unrelated to any particular microstructural basis, and may not always provide a satisfactory description. For example, the conservation of incompressibility during creep deformation is dubious in the presence of cavitation.

An explicit description of damage, given previously, may lead to a more appealing and physically-motivated expressions for the function  $f(n, \rho, x)$ . The most basic concept of our formalism is the definition of the macro material point. We summarize the discussed features of the latter:

- The macro material point has internal (microscopic) structure.
- The structure is the population of cracks.
- The matrix material is governed by constitutive equations (2.10)-(2.12).
- Dimensions of the macro material point must be large compared to the radius of an internal crack.

We observe that these features may be ideal *conceptual* ground for the classical continuum mechanics. A boundary-value problem can be specified, although it is not accessible for complete analysis. On the other hand, the presence of the function



$f(n, \rho, x)$  allows a description of the macro material point by three numbers  $n$ ,  $\rho$ , and  $x$ . Evidently function  $f(n, \rho, x)$  must be implicitly derived possibly, from a classical formulation. The following diagram helps to visualize characteristic relations.

Classical Continuum Mechanics



Homogenization



Continuum with Microstructure

The link between the two continuum theories is homogenization. In this work, the term homogenization has a conceptual meaning, although mathematicians (Sanchez-Palencia, 1980) reserve the term for a particular class of asymptotic procedures. Let us formulate a *possible* boundary-value problem corresponding to prescribed values of the arguments of the function.

Geometry. There are no topological restrictions on the exterior of the macro material point. We take a circular cylinder of volume  $V$  which contains  $N$  aligned planar penny-shaped cracks of radius  $a$ . The orthogonal coordinate system is given by the orthonormal triad of vectors  $e_i$ ,  $i = 1, 2, 3$ . The origin of the system coincides with the center of the cylinder. Vector  $e_1$  and the axis of the cylinder are aligned.

Crack planes are normal to  $\mathbf{e}_1$ , and the centers are given by sets  $\mathbf{x}^i$ ,  $i = 1, N$ . We implicitly presume that  $V \gg a^3$ .

Constitutive Equations. A response of a creeping matrix material is governed by equations (2.10)-(2.12).

Boundary Conditions. The cylinder is subjected to normal uniformly distributed tractions. The magnitude of the traction applied at the top and at the bottom is  $\sigma_1$ . The corresponding quantity for the side surface is  $\sigma_{-1}$ . We suppose that  $\sigma_1 \geq 0$ , and  $\sigma_1 \geq \sigma_{-1}$ . Crack faces are traction free.

The boundary-value problem must be completed by the equations of equilibrium and compatibility conditions.

The same physical situation may be interpreted in terms of a continuum with microstructure. The homogeneously loaded cylinder itself is the macro material point, cracks are accounted for by the crack density,  $\rho$ , and the tractions represent the macro stress tensor

$$\mathbf{T} = \sigma_1 \mathbf{e}_1 \otimes \mathbf{e}_1 + \sigma_{-1} (\mathbf{I} - \mathbf{e}_1 \otimes \mathbf{e}_1). \quad (3.3)$$

The triaxiality can be found from

$$x = \frac{\sigma_1}{\sigma_1 - \sigma_{-1}}. \quad (3.4)$$

The assumptions made about the population of cracks (see chapter 2), and the structure of the adopted stress tensor suggest that the response of the macro material point has to be axisymmetric.

In principle, the *ad hoc* choice of the material point boundary-value problem must be justified. We have to solve a truly three-dimensional problem ( $\sigma_1 \geq \sigma_2 \geq \sigma_3$ ), and demonstrate that the axisymmetric situation accurately reflects the general case.

Let us *imagine* that we obtain, by some means, the stress tensor field  $\mathbf{t}$ , which is the solution to the classical formulation. The volume average of the creep rate potential corresponding to this stress is equal to

$$F = \frac{1}{V} \int_V \frac{\sigma_0 \dot{\epsilon}_0}{n+1} \left( \frac{\bar{\sigma}}{\sigma_0} \right)^{n+1} dV. \quad (3.5)$$

The Mises stress in equation (3.5) is a field variable evaluated from the stress tensor  $\mathbf{t}$ . One of the key assumptions to make is that functions  $F$  defined microscopically, via (3.5), and macroscopically, via (2.15), are equal. This assumption implicitly relates  $f(n, \rho, x)$  to the local stress field. Tensor  $\mathbf{t}(\mathbf{T})$  can not be determined directly without actually solving the classical formulation. In general, any straightforward analytical approach to the boundary-value problem must fail. Nevertheless, some particular geometries and/or loadings allow for direct evaluations of the right-hand side integral. These cases can be interpreted in terms of the arguments of function  $f(n, \rho, x)$ .

First we consider a case of a small crack density. This situation may be realized if we fix the number of cracks and the volume, and decrease the crack radius. We assume that the radius is sufficiently small, such that *every* crack is embedded in a

large matrix. Alternatively, we say that the cracks do not interact. Thus the initial complicated geometry is completely decoupled, and reduced to what we term here as the *kernel* geometry. The latter is crucial for the rest of the chapter, therefore we feel that additional refinements are necessary.

The kernel boundary-value problem is the particular case of the previously formulated boundary-value problem:  $N = 1$ , and  $\mathbf{x}^1 = \mathbf{0}$  (Figure 3.1). This problem was treated in detail by He and Hutchinson (1983) for an arbitrary material exponent. The quantity implicitly related to function  $f(n, \rho, x)$  is the potential release,  $\mathcal{R}$ . It is defined as the difference between the integrals (3.5) calculated for the actual stress field and the homogeneous (crack is absent) stress field. In the limit of large volume, the crack radius becomes the only characteristic length scale. Functional form for  $\mathcal{R}$  can be taken similar to (2.15):

$$\mathcal{R} = a^3 R = \frac{\sigma_0 \dot{\epsilon}_0}{n+1} a^3 r(n, 0, x) \left( \frac{\bar{\sigma}}{\sigma_0} \right)^{n+1}. \quad (3.6)$$

We write a zero in the definition of function  $r(n, 0, x)$  as a tribute to earlier notational structure (2.15).

The creep rate potential for the cylinder with non-interacting cracks is equal to the sum of the individual contributions of the matrix and the cracks:

$$F \asymp F^{\text{matrix}} + \frac{N \mathcal{R}}{V}. \quad (3.7)$$

The first term of the right-hand side can be evaluated from equations (2.10)-(2.12). A combination of equations (2.9), (2.15), (3.6), and (3.7) gives us asymptotic behavior

of function  $f(n, \rho, x)$  for small crack densities

$$f(n, \rho, x) \asymp 1 + \rho r(n, 0, x). \quad (3.8)$$

Now let us investigate the behavior for small values of the triaxiality. The situation corresponds to a small magnitude of the axial traction relative to the lateral. If the axial traction is totally removed, the presence of the cracks notwithstanding, then with  $\sigma_1 = 0$  and  $x = 0$ , both damaged and undamaged materials should exhibit identical responses. The imposition of the continuity requires equations (2.18) being derivable from (2.10)-(2.12):

$$f'(n, \rho, 0) = 0. \quad (3.9)$$

We assume that function  $f(n, \rho, x)$  is sufficiently smooth, so Taylor's expansion is valid. Under this condition equation (3.9) results a small  $x$  asymptote:

$$f(n, \rho, x) \asymp 1 + \hat{\alpha}(n, \rho)x^2. \quad (3.10)$$

When both the crack density and the triaxiality are small, He and Hutchinson (1981) give a remarkable linearization for  $r(n, 0, x)$ . Detailed discussion of their solution is given in the next section, although the central idea is that at  $x = 0$ , the local stress field is homogeneous. This observation permits the formulation of an incremental problem for the linear, transversely isotropic solid, which can be solved in a closed-form. Hutchinson (1983) employs the linearization and gives

$$f(n, \rho, x) \asymp 1 + 4(n+1)\sqrt{\frac{n}{n+3}}\rho x^2, \quad \rho \rightarrow 0, \quad x \rightarrow 0. \quad (3.11)$$

Although we view the above expression only as an asymptotic, there is a substantial amount of recent research (Argon, et al, 1984, Tvergaard, 1985), in which (3.12) has been utilized with  $\rho$  representing a small, but finite crack density.

We recall that besides restrictions of this section, convexity conditions (2.17) must be imposed. Direct substitution of (3.11) into (2.17) gives us

$$1 - 4(n-1)\sqrt{\frac{n}{n+3}}\rho x^2 \geq 0. \quad (3.12)$$

It is obvious that for any finite value of the crack density, there should be some large  $x$ , such that convexity fails. This is an objection to using (3.12) as the final expression for  $f(n, \rho, x)$ .

Finally, we consider another extreme, "infinite triaxiality", which corresponds to microscopically isotropic stress. The absence of the deviatoric component, does not permit us employment of homogeneity in the sense of equations (2.15), (2.16). Instead, we may consider the case directly. The only possible way to construct the strain-rate potential is

$$F \propto \left(\frac{\text{tr} \mathbf{T}}{3}\right)^{n+1} = \sigma_1^{n+1} = x^{n+1} \bar{\sigma}^{n+1}, \quad x \rightarrow \infty, \quad \bar{\sigma} \rightarrow 0. \quad (3.13)$$

We argue this sequence heuristically rather than insisting upon it. The main reason for that is related to the resulting discontinuities for repeated eigenvalues of the stress tensor.

Let us summarize the proposed restrictions on the function.

I. As  $\rho \rightarrow 0, x \rightarrow 0$

$$f(n, \rho, x) \asymp 1 + 4(n+1)\sqrt{\frac{n}{n+3}}\rho x^2.$$

II. As  $\rho \rightarrow 0, \forall x$

$$f(n, \rho, x) \asymp 1 + \rho r(n, 0, x).$$

III. As  $x \rightarrow 0, \forall \rho$

$$f(n, \rho, x) \asymp 1 + \hat{\alpha}(n, \rho)x^2.$$

IV. As  $x \rightarrow \infty, \forall \rho$

$$f(n, \rho, x) \propto x^{n+1}.$$

V. As  $\forall x, \forall \rho$

$$ff'' - \frac{n}{n+1}f'^2 \geq 0, \quad f \geq 0.$$

The first three conditions must be compatible which, of course, defines limiting behavior of the functions  $\hat{\alpha}(n, \rho)$  and  $r(n, 0, x)$ . At the moment, we may accept or reject any candidates for the function on the basis of their compliance (or not) with this set of conditions. As a possible functional form we suggest

$$f(n, \rho, x) = \{1 + \alpha(n, \rho)x^2\}^{\frac{n+1}{2}}. \quad (3.14)$$

It is easy to show that all the requirements are satisfied if positive  $\alpha(n, \rho)$  (convexity) has the particular limit

$$\alpha(n, \rho) \asymp 8\sqrt{\frac{n}{n+3}}\rho, \quad \rho \rightarrow 0. \quad (3.15)$$

This expression then provides the more explicit

$$f(n, \rho, x) = \left\{ 1 + 8\sqrt{\frac{n}{n+3}}\rho x^2 + o(\rho)x^2 \right\}^{\frac{n+1}{2}}. \quad (3.16)$$

form for (3.14). Symbol  $o(\rho)$  designates all terms non-linear in  $\rho$ .

In order to gain some sense of the actual values of the parameters we can look at a simple tension test. We conclude, from equation (2.18), that for these conditions the axial strain rate is proportional to the function  $f$ . A rough estimate allows us to assume that fracture occurs when the strain rate increases by a factor of five, as compared to undamaged ( $\rho = 0$ ) material. As we expect positive contribution due to the higher order terms, then equation

$$\left( 1 + 8\sqrt{\frac{n}{n+3}}\rho_f \right)^{\frac{n+1}{2}} = 5, \quad x = 1,$$

should give us an "upper bound" for the critical crack density,  $\rho_f$ . For  $n = 5$ ,  $\rho_f \approx .112$ .

Another approximation of the critical crack density can be extracted from purely geometric considerations. For example, we assign an infinite hexagonal planar array to represent a polycrystalline structure. Intergranular fracture corresponds to a complete cavitation of any single set of the parallel boundaries. The critical crack density, appropriately redefined for a planar case, is  $\rho_f \approx .096$ .

Our quick calculations show that truncation error in  $\rho$  is not expected to be of serious importance <sup>1</sup>. Nevertheless, the amplification of the right-hand side of

---

<sup>1</sup>This statement presumes that the next terms in  $\rho$  is quadratic, or the function is sufficiently smooth. It turns out to be true within assumptions of the next sections.



equation (3.16) due to the power  $\frac{n+1}{2}$  may substantially involve higher order terms.

Therefore we must proceed further and adopt an approximate procedure for evaluating the higher order terms of expression (3.16).

## 3.2 Quantification via the Differential Self-Consistent Scheme

### 3.2.1 Background

The qualitative analysis entitles us with two major assumptions:

- The microscopically and the macroscopically defined creep rate potentials are numerically equal.
- Function  $f(n, \rho, x)$  may be represented by form (3.14), thus reducing our task to finding function  $\alpha(n, \rho)$ .

Any alternative to obtain  $\alpha(n, \rho)$  must be related to a homogenization. Any homogenization procedure is a compromise between physical soundness and mathematical convenience. The lack of stringent restrictions allows for a variety of *ad hoc* alternatives. We give the following loose classification of existing procedures:

- self-consistent methods
- bounding variational approaches
- periodic structures

- multiple interactions.

A broad class of self-consistent methods has been used extensively (see, for example, MacKenzie (1950), Hershey (1954), Kröner (1967), Budiansky and Wu (1962), Hill (1965a,b), and Mura (1982), who gives an extensive review.). The result central to these approaches is Eshelby's (1957) classical observation on ellipsoidal inclusions in infinite homogeneous elastic solid.

The works of Hashin (1962), and Hashin and Shtrikman (1963) initiated applications of variational principles for estimating bounds of material constants for inhomogeneous media. Willis (1982) summarizes more recent developments in this direction.

The so-called periodic structures have been attracting attention of mathematicians for the last decade (Sanchez-Palencia, 1980). The central idea of these procedures is an identification of a unit cell with the derivation of a macroscopic response from constitutive equations of the cell. Nemat-Nasser and Taya (1981) and Nemat-Nasser et al. (1982) effectively utilized a possibility of implementing Fourier series to composites with periodic structure.

A somewhat theoretical physics approach of what we refer to as multiple interactions has not received such an exhaustive attention of applied mechanicians as the prior methods. Recent developments are impressive asymptotic analysis of Chen and Acrivos (1978 a,b), and the two-volume monograph by Kunin (1982, 1983).

Major results in all these directions are essentially based on the linear elasticity framework. Nevertheless, there is an initiation of extensions towards understanding of non-linear materials (Hutchinson (1970), Duva (1985), Talbot and Willis (1985), Willis (1985)).

Although it is usually possible to make a correct choice of a procedure for a particular physical problem, this type of judgement has truly *a posteriori* nature. The absence of available experimental data suggests the adoption of a simple-to-implement homogenization procedure. We propose to employ the differential self-consistent scheme. It was suggested by Roscoe (1952) and generalized to tensorial forms by McLaughlin (1977). Let us motivate the basic idea behind the procedure. We consider two nearly identical isotropic bodies of volume  $V$ , subjected to macroscopic stress  $\mathbf{T}$ . The first body contains  $N + 1$  small cracks of radius  $a$ , which corresponds to damage  $\rho + \delta\rho$ . The second body has  $N$  cracks, and respectively damage  $\rho$ . The difference between the corresponding macroscopic potentials for the total volume is formally written as  $V\{F(\rho + \delta\rho, \mathbf{T}) - F(\rho, \mathbf{T})\}$ . On the other hand, in the *self-consistent* manner, we assume that this difference is equal to the potential release due to the introduction of a single crack into the *homogeneous* matrix characterized by  $F(\rho, \mathbf{T})$ :

$$V\{F(\rho + \delta\rho, \mathbf{T}) - F(\rho, \mathbf{T})\} = \mathcal{R}\{F(\rho, \mathbf{T}), \mathbf{T}\}. \quad (3.17)$$

The dimensional ground of equations (2.15) and (3.6) suggest the introduction of function  $r\{f(n, \rho, x), x\}$ . This function is related to the right-hand side of expression (3.17) via form (3.6). In the continuous limit for small values of  $\delta\rho$ , we obtain an ordinary differential equation:

$$\frac{\partial f(n, \rho, x)}{\partial \rho} = r\{f(n, \rho, x), x\}. \quad (3.18)$$

The obvious initial condition is  $f(n, 0, x) = 1$ .

A possible implementation of the scheme is better clarified via discrete equation (3.17):

1. We suppose that for a given crack density,  $\rho$ , function  $F(\rho, \mathbf{T})$  is known.
2. Solve the kernel problem for the potential release, thus find  $\mathcal{R}\{F(\rho, \mathbf{T}), \mathbf{T}\}$ .
3. Choose a value of  $\delta\rho$ , and obtain  $F(\rho + \delta\rho, \mathbf{T})$  from equation (3.17).
4. Return to the first step.

The algorithm is initiated by (2.10)-(2.12). It is important to realize that the ordinary differential equation views the stress tensor,  $\mathbf{T}$ , being macroscopically defined. Conversely, the boundary-value problem requires  $\mathbf{T}$  to be a local or microscopic quantity.

The rest of the chapter examines two ways of the coupled solution of the equations:

- A completely numerical treatment via a finite element representation of the kernel problem, and a Runge-Kutta discretization of equation (3.18).
- The possibility of a linearization of the kernel problem allows for a closed-form expression.

### 3.2.2 Numerical Analysis

A numerical treatment of the problem falls into two parts: integration of equation (3.18) and development of a routine for the kernel geometry with the arbitrary material model.

Basic tools behind integration of an ordinary differential equation of the first order are fairly well understood. We want to emphasize some specific features of the particular problem. Let us substitute (3.14) into (3.18)

$$\frac{n+1}{2} \{1 + \alpha(n, \rho) x^2\}^{\frac{n-1}{2}} x^2 \frac{\partial \alpha}{\partial \rho} = r(f, x), \quad \forall x. \quad (3.19)$$

If functional form (3.14) is exact, then we should be able to obtain the unique  $\alpha(n, \rho)$  for all triaxialities. As expression (3.14) is an approximation, we have to expect, in general, the absence of the uniqueness. Let us suppose that for a given set of  $x_i$  we solve (3.19), and obtain the corresponding set  $\alpha_i(n, \rho)$ . We define  $\alpha(n, \rho)$  in a least square sense via

$$\sum_i \left\{ (1 + \alpha_i(n, \rho) x_i^2)^{\frac{n+1}{2}} - (1 + \alpha(n, \rho) x_i^2)^{\frac{n+1}{2}} \right\}^2 = \min. \quad (3.20)$$

The derivative of the left-hand side with respect to  $\alpha_i$  must be equal to zero, thus we have an algebraic expression for  $\alpha(n, \rho)$ . Of course, we presume that functions  $\alpha_i$  are sufficiently close, otherwise we must question validity of (3.14).

Let us fix both,  $x$  and  $n$ , so that equation (3.19) may be considered as being "very" ordinary. Probably the most characteristic feature of the equation is substantial complexity associated with an evaluation of the right-hand side. Namely, every value of  $r(f, \rho)$  requires an independent solution of the kernel problem. Therefore, we must be especially interested in reducing the number of the right-hand side evaluations. Unfortunately, the *a priori* optimal numerical method for ordinary differential equations does not exist. Nevertheless, we can claim that an *explicit* integration allows us to *prescribe* a number of  $r(f, x)$  computations. The drawback of the explicit procedures is the instability, or error accumulation (for a detailed treatment see Dahlquist et al., 1974), therefore a convergency test is essential. A popular choice is a fourth order Runge-Kutta scheme:

$$\begin{aligned}
 k_1 &= (\delta\rho)r(f, x) \\
 k_2 &= (\delta\rho)r\left(f + \frac{1}{2}k_1, x\right) \\
 k_3 &= (\delta\rho)r\left(f + \frac{1}{2}k_2, x\right) \\
 k_4 &= (\delta\rho)r(f + k_3, x) \\
 f(n, \rho + \delta\rho, x) &= f + \frac{k_1 + 2k_2 + 2k_3 + k_4}{6}.
 \end{aligned}
 \tag{3.21}$$

The above algorithm written in terms of functions  $f$  and  $r$ , because for a fixed  $x$ , differential equations (3.18) and (3.19) are interchangeable. Equations (3.21) take advantage of the implicit dependence of  $r(f, x)$  upon the crack density,  $\rho$ . The truncation error of scheme (3.21) is  $O\{(\delta\rho)^4\}$ .

We employ a finite element method to compute function  $r(f, x)$ . All computations reported herein have been performed using the ABAQUS finite element version 4-5-159 program on a DATA GENERAL MV-100000 computer. The justification for these particular tools is: versatility of the method, flexibility of the program, and availability of the computer.

The finite element mesh is shown in *Figure 3.2* The choice of the mesh is dictated by two factors: first, the mesh must be fine enough to provide us with an accurate discretization; secondly, as we have to model an infinite matrix via finite geometry, we must be sure that the radius of the cylinder is large enough compared to the crack radius. We have conducted the following tests for *incompressible* materials:

1. For linear material,  $n = 1$ , the numerical and the closed-form (Sneddon, 1964) solutions agree to the first four significant digits.
2. For non-linear materials ( $n = 3, 5, 8$ ), and combined loadings ( $x=1, 2, 3, 4, 5$ ) the increase of the external radius from the present  $20a$  to  $30a$  did not change the potential release rate by more than a half of a percent.
3. For the same  $x$  and  $n$  as in the second test, a refinement of mesh (the number of

elements was approximately doubled) did not detect errors above one percent.

The potential release is the key quantity of the analysis; therefore we feel obliged to comment on its evaluation. The current approach is straightforward, within the ABAQUS environment. The simple one length-scale geometry provides a relationship between potential release and the path-independent integrals (Budiansky and Rice, 1973, Budiansky and O'Connell, 1976):

$$\mathcal{R} = \frac{3}{2} \pi a^2 J. \quad (3.22)$$

In the above expression  $J$  is Rice's integral (Rice, 1968). Computation of  $J$  is a standard procedure of the program via the virtual crack extension method (Parks, 1977).

The eight node, displacement based axisymmetric element with reduced integration (ABAQUS element type CAX8R) gives desired accuracy combined with substantial economy. The far field axisymmetric stresses are applied in a manner such that  $\sigma_1 = 1$ , and  $\sigma_{-1}$  takes values to give a prescribed triaxiality.

Constitutive response is modeled via user defined subroutine UMAT. The subroutine is called for every material point, and for a given strain rate tensor it computes the stress and the stiffness tensors. The existence of the Legendre transform (section 2.2) allows for a straightforward coding of algebraic expressions (Rodin and Parks, 1986b)

Two series of numerical experiments were conducted. In the first set of com-



putations we fix the triaxiality at pure tension ( $x = 1$ ), and determine  $\alpha(n, \rho)$  for three values of material exponent  $n = 3, 5, 8$ . The artificial termination condition was taken in a form

$$f(n, \rho_f, 1) = 5.$$

Convergence studies show that for the first two material exponents the pointwise differences between  $\alpha(n, \rho)$ , corresponding to steps  $\delta\rho = .01$  and  $\delta\rho = .02$ , did not exceed one percent. For  $n = 8$ , we adopted the step  $\delta\rho = .01$ , without any additional convergency tests. The second set of computations employs the least square procedure for the triaxiality varying from one to five with increment of one. For the lower exponents, the step  $\delta\rho = .02$  gives the least square error in  $\alpha(n, \rho)$  below six percent. Unfortunately, we were not able to generate similar results for  $n = 8$ , because complexity of computations increased with higher values of  $x$  and  $n$ . We postpone our discussion of the results till the end of the chapter.

### 3.2.3 Linearized Solution

First, we would like to raise the question: "Do we really need a linearization, if a complete numerical procedure is available?" We give three major reasons for the positive response:

- A linearized solution gives us simple continuous representation of functions, otherwise given via limited discrete databases.
- A linearized solution may reveal some important analytical properties.

- I think, that the idea of having reasonable closed-form expression for these class of problems is extremely exciting *per se*.

The starting point of the linearization is the existence of a homogeneous non-trivial stress field. We have mentioned already that the macroscopic stress tensor  $\mathbf{T}^0 = \sigma_{-1}(\mathbf{I} - \mathbf{e}_1 \otimes \mathbf{e}_1)$ ,  $\sigma_{-1} < 0$ , does generate this kind of field, notwithstanding the cracks' presence. The application of a *small* axial traction,  $\sigma_1$ , may be viewed as a perturbation of the preexisting field. The last assumption motivates a formulation of a *linear* boundary-value problem. A complete solution corresponding to a general axisymmetric stress tensor,  $\mathbf{T} = \sigma_1 \mathbf{e}_1 \otimes \mathbf{e}_1 + \sigma_{-1}(\mathbf{I} - \mathbf{e}_1 \otimes \mathbf{e}_1)$ , is a combination of the homogeneous and the linear solutions. He and Hutchinson (1981) presented the linearized solution for the single crack in the undamaged matrix material. We follow their methodology, and suggest an extension by incorporating it into the differential self-consistent scheme. This extension is possible due to the presence of a robust analytical approach to the kernel problem within an anisotropic elasticity (Hoenig, 1977).

We can motivate the linearization within the context of equation (3.19). For small  $x$ , the left hand-side is asymptotically equal to  $\frac{n+1}{2} x^2 \frac{\partial \alpha}{\partial \rho}$ . On dimensional ground we can claim that the energy release rate,  $\mathcal{R}$ , must be quadratic in  $\sigma_1$ , and proportional to  $\sigma_{-1}^{n-1}$ . The former is a direct result of the linearity of the perturbation, while the latter characterizes compliance of the homogeneous field. It

is easy to verify that for small triaxialities the leading term of the right-hand side is proportional to  $x^2$ . Thus, if  $x$  is small, equation (3.19) should give us asymptotically unique  $\alpha(n, \rho)$  for all triaxialities. The initial condition is  $\alpha(n, 0) = 0$ .

Let us address some details of the linear solution. The surrounding material can be described via a compliance tensor, which is derived as the second derivative of the creep rate potential with respect to the stress tensor, at point  $\mathbf{T}^{(0)}$ . We prefer the notation of Hoenig (1977), and write the compliance matrix rather than the tensor. The matrix relates the vector of the *local* stresses,  $\{\sigma_{11}, \sigma_{22}, \sigma_{33}, \sigma_{12}, \sigma_{13}, \sigma_{23}\}$  to the corresponding vector of the *local engineering* strains. Naturally, the first direction coincides with the *global*  $\mathbf{e}_1$ , while the other two must complete the triad. The matrix represents a transversely isotropic linear material, with the axis of the material symmetry along  $\mathbf{e}_1$ :

$$\mathcal{L} = \begin{bmatrix} \alpha + n & -\frac{n}{2} & -\frac{n}{2} & 0 & 0 & 0 \\ 0 & \frac{n+3}{4} & \frac{n-3}{4} & 0 & 0 & 0 \\ 0 & 0 & \frac{n+3}{4} & 0 & 0 & 0 \\ 0 & 0 & 0 & 3 & 0 & 0 \\ 0 & 0 & 0 & 0 & 3 & 0 \\ 0 & 0 & 0 & 0 & 0 & 3 \end{bmatrix} \frac{\dot{\epsilon}_0}{\sigma_0} \left( -\frac{\sigma_{-1}}{\sigma_0} \right)^{n-1}. \quad (3.23)$$

We will write letter H with equation numbers to designate the corresponding expression of Hoenig (1977). A set of elastic material functions or constants is defined (26H) via

$$\frac{1}{E} := \frac{\dot{\epsilon}_0}{\sigma_0} \left( -\frac{\sigma_{-1}}{\sigma_0} \right)^{n-1} \frac{n+3}{4},$$

$$\frac{1}{H} := \frac{4(n+\alpha)}{n+3},$$

$$\nu_1 := \frac{3-n}{n+3},$$

$$\nu_2 := \frac{2n}{n+3}.$$

An expression for the potential release rate can be extracted from a combination of equations (7H, 27H, 30H):

$$\mathcal{R} = \frac{4\sqrt{2}a^3\sigma_1^2}{3E} \sqrt{\frac{1}{H} - \nu_2^2} \sqrt{(1+\nu_1)(1-\nu_2) + \sqrt{(1-\nu_1^2)(\frac{1}{H} - \nu_2^2)}}. \quad (3.24)$$

Finally, differential equation (3.18) can be rewritten

$$\frac{d\alpha}{d\rho} = \frac{2\sqrt{2}(n+3)}{3} \sqrt{\frac{1}{H} - \nu_2^2} \sqrt{(1+\nu_1)(1-\nu_2) + \sqrt{(1-\nu_1^2)(\frac{1}{H} - \nu_2^2)}}. \quad (3.25)$$

Ordinary differential equation (3.25) can be integrated in quadratures. Fairly tedious and straightforward algebra gives us the answer:

$$\alpha(n, \rho) = 8\sqrt{\frac{n}{n+3}}\rho + \frac{16(2n+3)}{n+3}\rho^2 + \frac{64}{9}\sqrt{\frac{n}{n+3}}\rho^3 + \frac{64n}{27(n+3)}\rho^4. \quad (3.26)$$

Naturally, the formula is compatible with the dilute asymptotics.

### 3.2.4 Comparison of the Analyses.

We have performed both numerical and analytical analyses of the problem. The numerical procedure must be more accurate, as it solves the kernel problem “exactly”. On the other hand, the analytical expression is much more attractive for application, and of course, does not lack a somewhat luring beauty. Analytical form (3.16) can be considered a dilute solution. Expression (3.16) has the advantage of

providing very simple estimates. In general, this estimate requires only one solution of a single crack (maybe any defect) in the undamaged power-law matrix.

*Figures 3.1, 3.2, 3.3* show alternative presentations of results for material exponents,  $n = 3, 5, 8$ , respectively. We measure  $\rho$  on the horizontal axis, and  $f(n, \rho, 1)$  on the vertical axis. Function  $f(n, \rho, 1)$  may be interpreted as the ratio of the axial strain rate in tension to the axial strain rate in compression, in a simple tension test. Here we presume that the compressive tractions do not cause cavitation, thus material remains being undamaged in the process of deformation.

There are four curves in the first two figures:

1. Finite element calibrations based on the single,  $x = 1$ , test.
2. The linearized solution.
3. Finite element calibrations based on the least squares procedure,  $x = 1, 2, 3, 4, 5$ .
4. The dilute solution.

Although the numerical curves involve more rigorous analysis of the kernel problem, there is still the arbitrary factor involved, namely, the choice of  $x = 1$  for the first curve, or the fitting set for the second curve. It is fair to say, that any arguments about ultimate preference of one curve over the other are vulnerable. The important conclusion, I think, is rather small difference in the predictions of the four analyses. We prefer to avoid any possible speculations without additional parametric studies.

*Figure 3.5* presents the results for  $n = 8$ . The least square analysis for the prior chosen set is missing. The reason is the eventual deterioration of numerical conditioning of the boundary-value problem, with the increasing values of the triaxiality and the material exponent. Of course, we could have chosen another least squares set, but tendencies of the curves on all three figures are very similar. Therefore, we do not expect any dramatic changes in conclusions in the presence of the analysis.

We want explicitly state two propositions:

- The linearization provides a sensible alternative to the fully numerical implementation of the differential self-consistent scheme, thus we adopt expression (3.26) being “the” answer.
- The dilute solution (3.16) is an acceptable quick estimate. It is a straightforward way to extend this functional form to more topologically sophisticated models of damage.

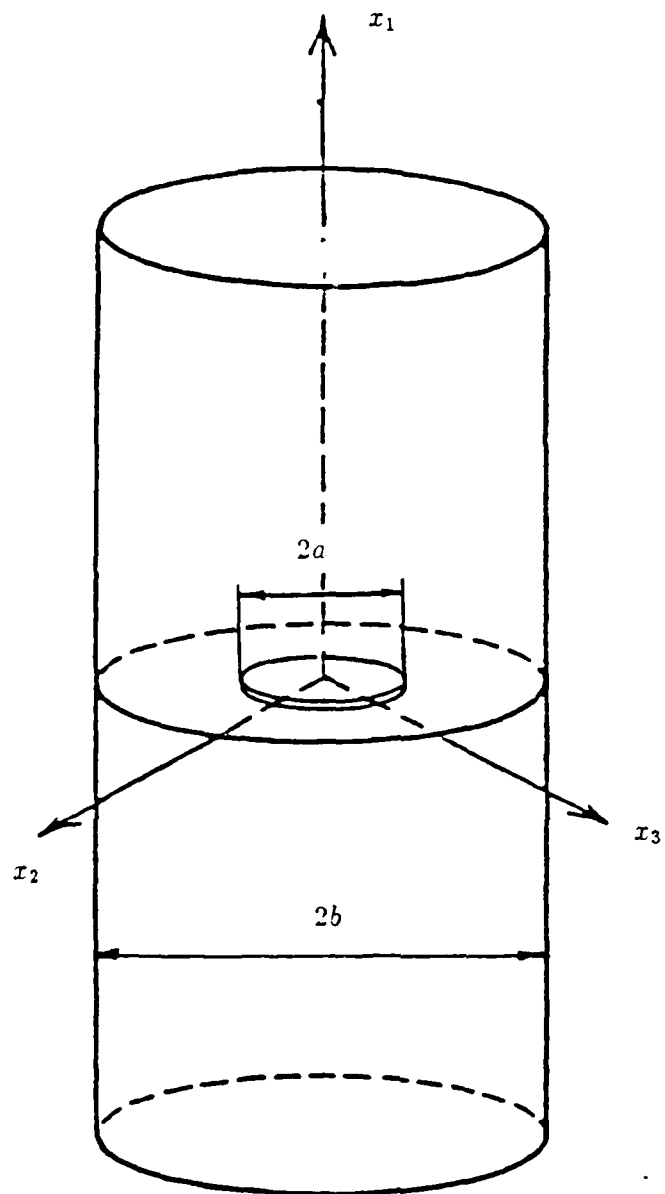


*Figure 3.1* Circular Cylinder with a Penny-Shaped Crack

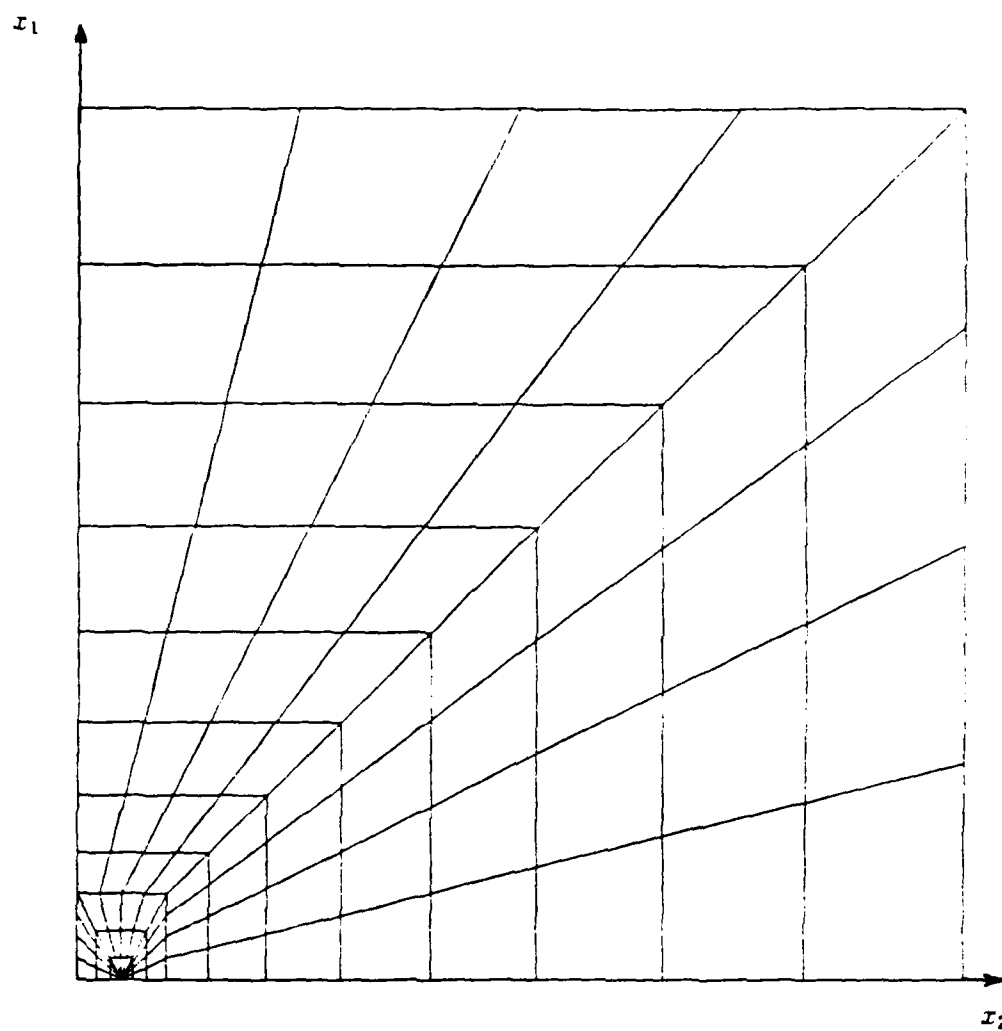


Figure 3.2 Finite Element Mesh



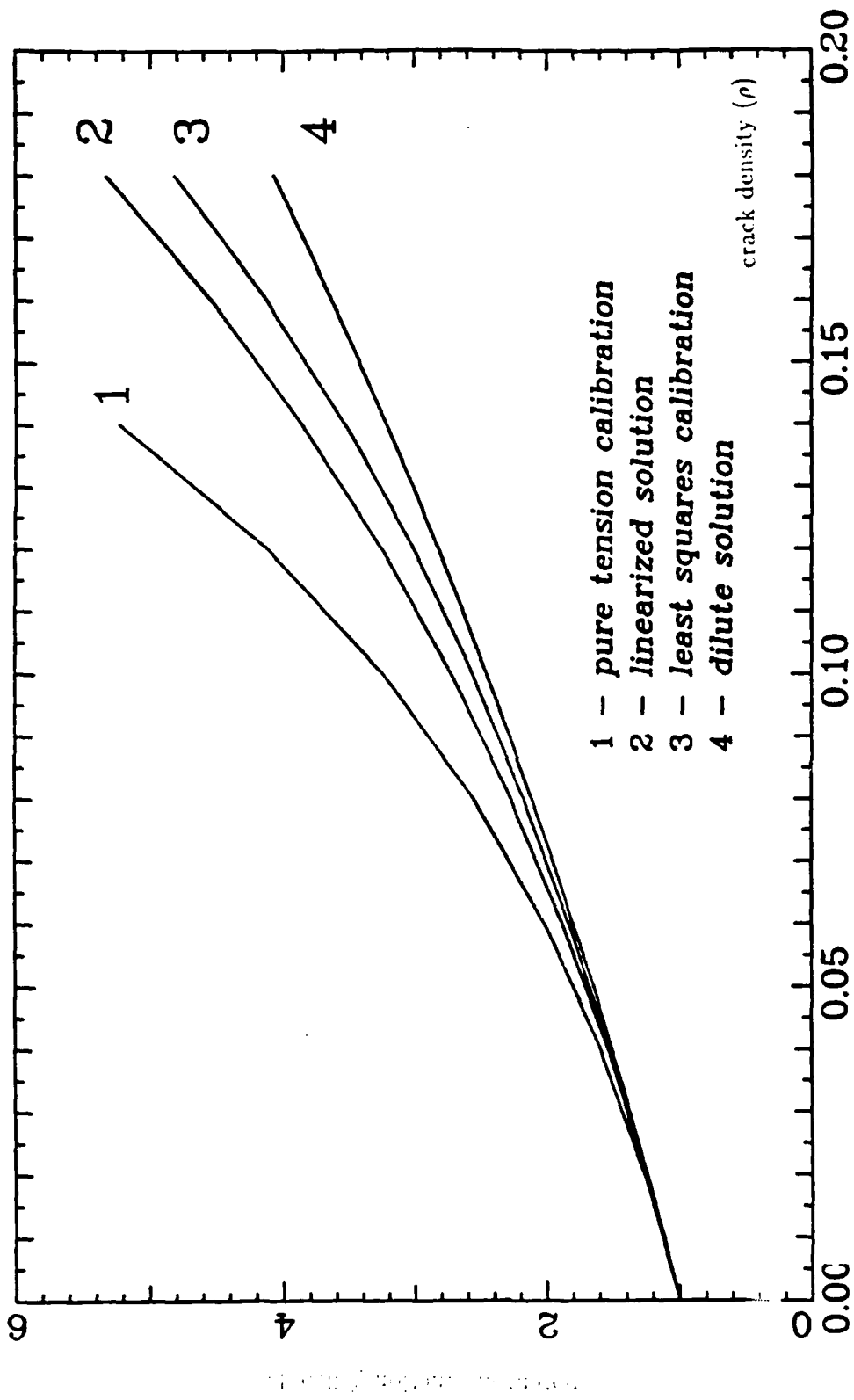


Figure 3.8 Dependence of potential function  $f(\nu, \rho, x)$  on the crack density for the case of a pure tension ( $x = 1$ ) and material exponent ( $n = 3$ )

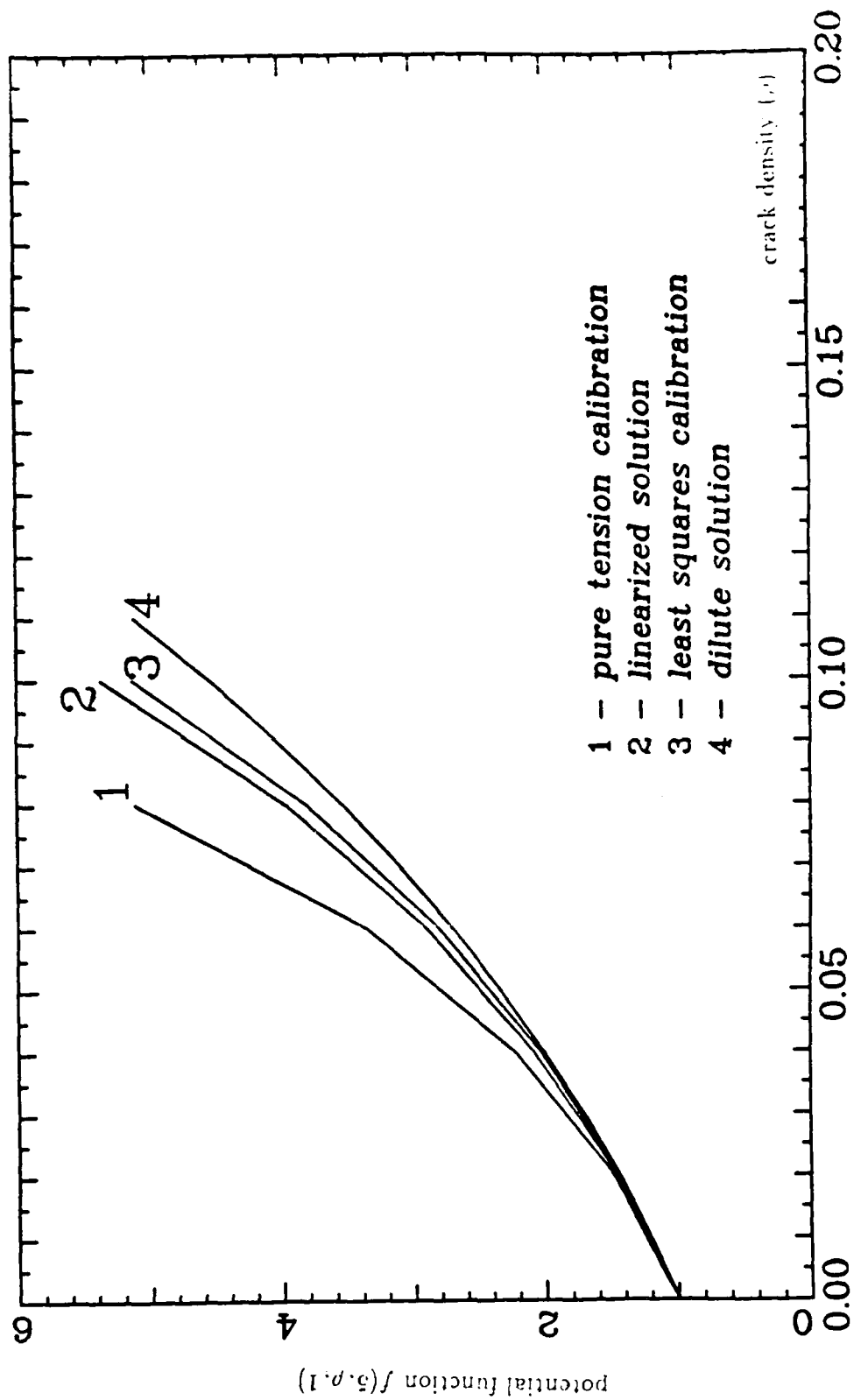


Figure 3.4 Dependence of potential function  $f(n, \rho, x)$  on the crack density for the case of a pure tension ( $x = 1$ ) and material exponent ( $n = 5$ )

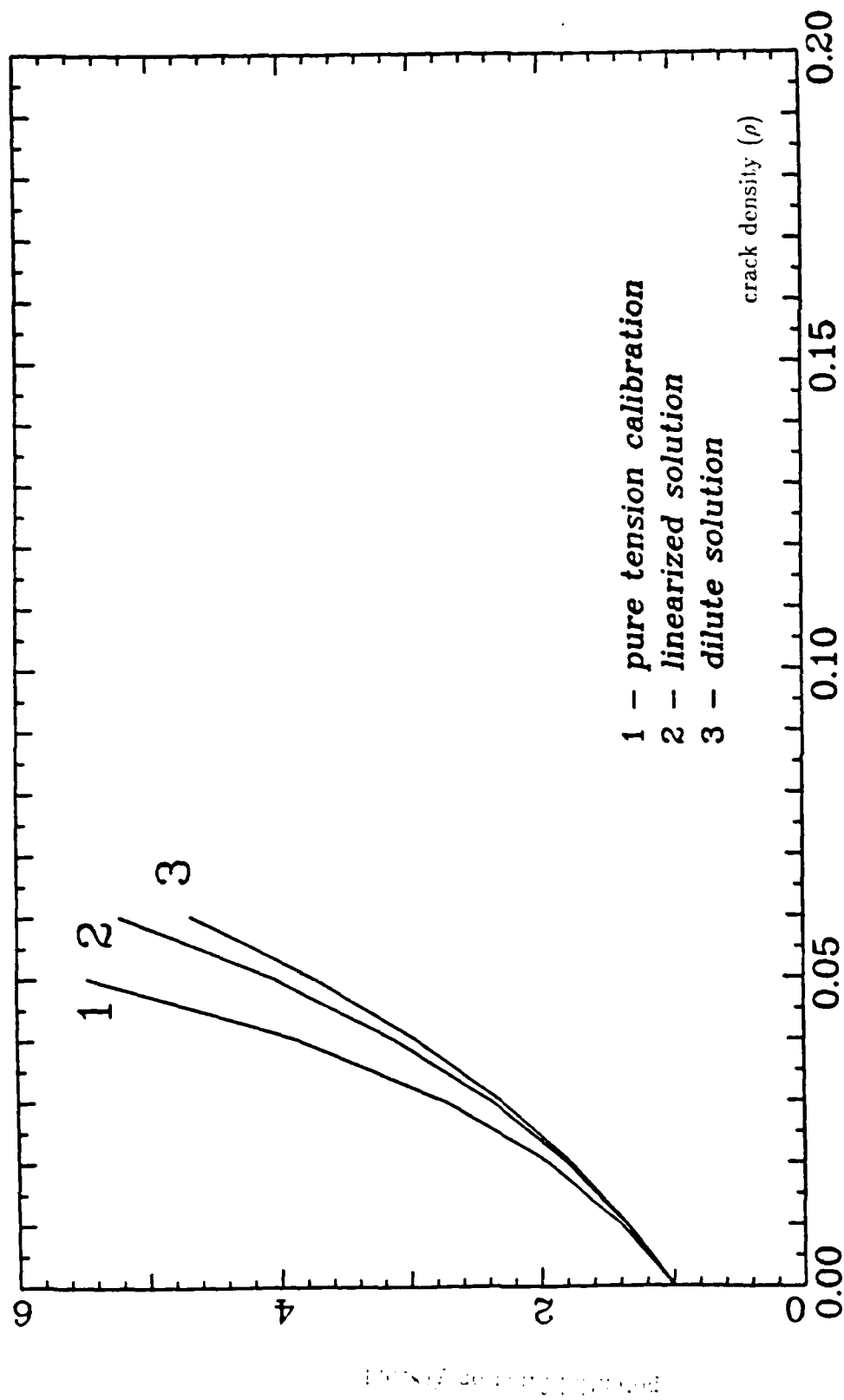


Figure 9.5 Dependence of potential function  $f(n, \rho, x)$  on the crack density for the case of a pure tension ( $x = 1$ ) and material exponent ( $n = 8$ )

## Chapter 4

### Discussion

This chapter highlights some essential and, perhaps, sensitive points of this research. We take some liberty allowing sometimes rather subjective propositions;<sup>1</sup> therefore some statements are semi-speculative.

The introductory chapter centers on phenomenological and metallurgical approaches to creep deformation. It seems that a combination of the power-law and Monkman-Grant relations, poses a very serious challenge to any proposed constitutive model for creep. Current phenomenological models have the attractive feature of being simple and adequately accurate. Development of more sophisticated models usually involves a mixture of applied mechanics and metallurgy. The Continuum Damage Mechanics of Kachanov-Rabotnov-Leckie-Hayhurst is a direct extension of phenomenological ideas to the internal variable structure. "Right" power-law functional forms, sufficient flexibility to fit data, and most importantly the presence of powerful software and hardware are central for structural applications. The draw-

---

<sup>1</sup>If we have not done it already.

back of the theory is the absence of a physical definition of damage, but a lot of design problems can be resolved without addressing microscopic mechanisms. Thus, if model parameters may be determined such that the theory accurately represents material behavior, we have reached our goals. The model of Hutchinson (1983) gives the damage parameter an explicit physical interpretation. Tveergard (1985) combined this model with existing micromechanical developments, and incorporated the combination into an internal variable framework. His work is a remarkable collection of the efforts of many investigators into a single model. Argon et al. (1984) present a comprehensive formulation, and their work is probably the first to utilize two state variables to describe both dislocations structure and intergranular cavitation. Our model uses the same internal variable formulation with a greater concentration on continuum mechanics.

Let us address some technical aspects of the model. Equations (2.1)-(2.7) is a canonical form of the internal variable framework, and this system may be viewed within the context of optimal control theory. We associate the state with the creep strain tensor and the internal state, and the stress tensor is the input. A standard formulation of optimal control theory is completed by a functional, and a stationary point of the functional corresponds to an optimal input. Currently, we do not see any transparent implementation of this approach to a sensible physical problem, nevertheless powerful mathematical tools of optimal control theory and variational

calculus may open flourishing grounds for research.

It is essential to bear in mind the conceptual importance of homogenization. Although ideas of homogenization are central to any description utilizing continuous description, many authors fail to acknowledge this fact. Micromechanical formulations do require clear physical interpretation of all the physical parameters. Straightforward definition of damage may lead to somewhat ambiguous conclusions, and tensorial damage states must be *explicitly* justified, especially in the sense of their algebras.

The tensorial representation is a very interesting problem *per se*. The structure of equations resembles both the power-law incompressible model and linear elasticity. The conjugateness between the maximum principal stress and the rate of creep dilatation is simply charming. A more interesting topic for *discussion* is the introduction of invariants  $\sigma^{(p)}$ . The motivation behind the invariants is the requirement of non-singular constitutive equations. The singularity arises as a direct consequence of the non-symmetric utilization of the principal stresses in the formulation. A similar situation occurs in plasticity. The Tresca hexagon is based on the absolute difference between the maximum and the minimum principal stresses, and the absence of the intermediate stress induces the singularity. In both cases constitutive relations are based on a limited experimental data. For example, combined tension and torsion tests (Trampczynsky et al., 1981) implicitly suggest interprete-

ing tensile stress as the maximum principle stress. We can eliminate ambiguities through a three-dimensional experimental program. The straightforward proposition of fitting experimental data with the Mises stress, and an appropriately chosen  $\sigma^{(p)}$  (some kind of a least squares procedure) has a drawback. The invariant is a non-homogeneous function of the stress tensor, and we lose many analytical advantages.

The qualitative analysis is motivated by He and Hutchinson's (1981) work. It seems that we have "squeezed" all possible information from the continuum formulation, but it is very important to remember that we lack asymptotes at the critical crack density, which essentially classifies the material model as "creeping compressible", rather than "creeping damaged". Fortunately, functional form (3.15) can be extended to include singular behavior at fracture. This extension is a possible topic for our future research.

Functional forms (3.15) and (3.26) suggest, that the material exponent and the triaxiality are very important, if we want to extend the meaning of dilute population of cracks from a purely geometric quantity to a constitutive response. More creep ductile materials exhibit higher sensitivity to the presence of cracks and high triaxialities.

The other important question in the qualitative analysis is a choice of the kernel problem. The initial He and Hutchinson (1981) axisymmetric boundary-value

problem has not encountered any serious objections so far. Currently, we are in a process of analysis of the three-dimensional kernel problem.

The differential self-consistent scheme has enabled us to conduct both, the finite element and the linearized analyses. It is a convenient and sensible tool, which lead to expression (3.26), and thus to a completion of the homogenization.

Finally, we would like to comment on the initially proposed damage model adopted by Rice (1981), Anderson and Rice (1985), and Tvergaard (1985). Namely, we have to take into account the individual local tractions. We consider the case of equal local traction on every crack. The adoption of the linearization suggests that the combined action of the axial macrostress,  $\sigma_1$ , and the local tractions,  $\sigma_{loc}$ , can be accounted in a straightforward way:

$$x := \frac{\sigma_1 - \sigma_{loc}}{\bar{\sigma}}.$$

The above redefinition has been suggested already, but the linearization makes it more convincing.



## Bibliography

- [1] Anderson, P.E., Rice, J.R., (1985), 'Constrained Creep Cavitation of Grain Boundary Facets,' *Acta Metallurgica*, Vol. 33, p. 409.
- [2] Argon, A.S., Chen, I.W., Law, C.W., (1980), 'Intergranular Cavitation in Creep: Theory and Experiments,' in *Creep-Fatigue-Environment Interactions*, ed. R.M. Pelloux and N.S. Stoloff, AIME, N.Y., p. 46.
- [3] Argon, A.S., (1982), 'Mechanisms and Mechanics of Fracture in Creeping Alloys,' in *Recent Advances in Creep and Fracture of Engineering Materials and Structures*, eds. B. Wilshire and D.R.J. Owen, Pineridge Press, Swansea, U.K., p. 1.
- [4] Argon, A.S., Lau, C.W., Ozmat, B., Parks, D.M., (1984), 'Creep Crack Growth in Ductile Alloys,' in *Fundamentals of Deformation and Fracture*, ed., K.J. Miller, Cambridge University Press, p. 189.
- [5] Argon, A.S., Bhattacharya, A.K., (1986), 'Primary Creep in Nickel: Experiments and Theory,' to be published.

- [6] Ashby, M.F., Dyson, B.F., (1984), 'Creep Damage Mechanisms and Macromechanics,' National Physics Laboratories Report.
- [7] Ashby, M.F., Gandhi, C., Taplin, D.M.R., (1979), 'Fracture-Mechanism Maps and their Construction for F.C.C. Metals and Alloys,' *Acta Metallurgica*, Vol. 27, p. 699.
- [8] Bird, J.E., Mukherjee, A.K., Dorn, J.E., (1969), '*Qualitative Relations between Properties and Microstructure*,' ed. Brandon, D.G., Rosen, A., Israel University Press, p. 255.
- [9] Budiansky, B., Wu, T.T., (1962), 'Theoretical Predictions of Plastic Strains of Polycrystals,' *Proceedings 4th U.S. National Congress of Applied Mechanics*, p. 1175.
- [10] Budiansky, B., O'Connell, R.J., (1976), 'Elastic Moduli of a Cracked Solid,' *International Journal of Solids and Structures*, Vol. 12, p. 81.
- [11] Budiansky, B., Hutchinson, J.W., Slutsky, S., (1981), 'Void Growth and Collapse in Viscous Solids,' *Mechanics of Solids, The Rodney Hill 60th Anniversary Volume*, ed. H.G. Hopkins and M.J. Sewell, Pergamon Press, Oxford, p. 13.
- [12] Budiansky, B., Rice, J.R., (1973), 'Conservation Laws and Energy Release Rates,' *Journal of Applied Mechanics*, Vol. 40, p. 201.

- [13] Brown, A.M., Ashby, M.F., (1980), 'On the Power-Law Creep Evolution,' *Scripta Metallurgica*, Vol. 14, p. 1297.
- [14] Carlson, D.E., Hoger, A., (1984), 'The Derivative of a Tensor-Valued Function of a Tensor,' Institute for Mathematics and its Applications, IMA Preprint Series 101.
- [15] Chen, H.S., Acrivos, A., (1978a), 'The Solution of the Equations of Linear Elasticity for an Infinite Region Containing Two Spherical Inclusions,' *International Journal of Solids and Structures*, Vol. 14, p. 331.
- [16] Chen, H.S., Acrivos, A., (1978b), 'The Effective Elastic Moduli of Composite Materials Containing Spherical Inclusions at Non-Dilute Concentrations,' *International Journal of Solids and Structures*, Vol. 14, p. 349.
- [17] Chen, I.W., Argon, A.S., (1981), 'Creep Cavitation in 304 Stainless Steel,' *Acta Metallurgica*, Vol. 29, p. 1321.
- [18] Cocks, A.C.F., Ashby, M.F., (1982), 'On Creep Fracture by Void Growth,' in *Progress in Materials Science*, Vol. 27, p. 189.
- [19] Dahlquist, G., Björsk, Å., Anderson, N., (1974), *Numerical Methods*, Prentice-Hall, Inc., Englewood Cliffs, New Jersey.
- [20] Duva, J.M., Hutchinson, J.W., (1983), 'Constitutive Potentials for Dilutely Voided Nonlinear Materials,' *Mechanics of Materials*, Vol. 31, p. 41.

- [21] Duva, J.M., (1985), 'A Self-Consistent Analysis of the Stiffening Effect of Rigid Inclusions on a Power-Law Material,' Journal of Engineering Materials and Technology, Vol. 106, No. 4, p. 317.
- [22] Duva, J.M., (1986), 'A Constitutive Description of Non-Linear Materials Containing Voids,' Harvard University Report.
- [23] Eshelby, J.D., (1957), 'The Determination of the Elastic Field of an Ellipsoidal Inclusion, and Related Problems,' Proceedings of Royal Society, London Series, Vol. A241, p. 376.
- [24] Evans, H.E., (1984), '*Mechanisms of Creep Fracture*,' Elsevier Applied Science Publishers, London, New York.
- [25] Frost, H.J., Ashby, M.F., (1982), Deformation-Mechanism Maps. The Plasticity and Creep of Metals and Ceramics, Pergamon Press.
- [26] Grant, N.J., Mullendore, A.W., (1965), '*Deformation and Fracture at Elevated Temperatures*,' MIT Press, Cambridge, Massachusetts.
- [27] Hashin, Z., (1962), 'The Elastic Moduli of Heterogeneous Materials,' Journal of Applied Mechanics, Vol. 29, p. 143.
- [28] Hashin, Z., Shtrikman, S., (1963), 'A Variational Approach to the Theory of the Elastic Behavior of Multiphase Materials,' Journal of Mechanics and Physics of Solids, Vol. 11, p. 127.

- [29] Hayhurst, D.R., (1983), 'On the Role of Creep Continuum Damage in Structural Mechanics,' in *Engineering Approaches to High-Temperature Design*, ed. Wilshire, B., Owen, D.R.J., Swansea, U.K., p. 85.
- [30] Hayhurst, D.R., Leckie, F.A., (1983), 'Behavior of Materials at High Temperatures,' *Proceedings of Fourth International Conference on Mechanical Behavior of Materials*, Stockholm, Vol. 2, p. 1195.
- [31] Hayhurst, D.R., Brown, P.R., Morrison, C.J., (1983), 'The Role of Continuum Damage in Creep Crack Growth,' *Philosophical Transactions of Royal Society*, London, Vol. A311, p. 131.
- [32] He, M.Y., Hutchinson, J.W., (1981), 'The Penny-Shaped Crack and the Plain Strain Crack in an Infinite Body of Power-Law Material,' *Journal of Applied Mechanics*, Vol. 48, p. 830.
- [33] He, M.Y., Hutchinson, J.W., (1983), 'Bounds for Fully Plastic Crack Problems for Infinite Bodies, *Elastic-Plastic Fracture: Second Symposium*, Vol.1 - *Inelastic Crack Analysis*. ASTM STP 803, C.F. Gudas, eds., American Society for Testing and Materials, Philadelphia, p. 1277.
- [34] Hershey, A.V., (1954), 'The Elasticity of an Isotropic Aggregate of an Anisotropic Cubic Crystals,' *Journal of Applied Mechanics*, Vol. 21, p. 236.
- [35] Hill, R., (1965a), 'Continuum Micro-Mechanics of Elastoplastic Polycrystals,'

Journal of Mechanics and Physics of Solids, Vol. 13, p. 89.

- [36] Hill, R., (1965b), 'A Self-Consistent Mechanics of Composite Materials,' Journal of Mechanics and Physics of Solids, Vol. 13, p. 213.
- [37] Hoehing, A., (1977), 'Elastic and Electrical Moduli of Non-Randomly Cracked Bodies,' PhD Thesis, Harvard University.
- [38] Hutchinson, J.W., (1970), 'Elastic-Plastic Behavior of Polycrystalline Metals and Composites,' Proceedings of Royal Society, London Series, Vol. A319, p. 247.
- [39] Hutchinson, J.W., (1983), 'Constitutive Behavior and Crack Tip Fields for Materials Undergoing Creep-Constrained Grain Boundary Cavitation,' Acta Metallurgica, Vol. 31, p. 1079.
- [40] Johnson, A.E., Henderson, J., Khan, B., (1962), *Complex-Stress, Creep, Relaxation and Fracture of Metallic Alloys*, Her Majesty's Stationery Office, Edinburgh.
- [41] Kachanov, L.M., (1958), 'Time of the Fracture Process under Creep Conditions,' Izvestiya Akademii Nauk SSSR, Vol. 8, p. 26.
- [42] Krajcinovic, D., (1983), 'Creep of Structures - A Continuous Damage Approach,' Journal of Structural Mechanics, Vol. 11, p. 1.

- [43] Kröner, E., (1967), 'Elastic Moduli of Perfectly Disordered Composite Materials,' *Journal of Mechanics and Physics of Solids*, Vol. 15, p. 319.
- [44] Kunin, I.A., (1982) '*Mechanics of Continuum with Microstructure. Part I - One-Dimensional Models*,' Springer-Verlag, New York.
- [45] Kunin, I.A., (1983) '*Mechanics of Continuum with Microstructure. Part II - Three-Dimensional Models*,' Springer-Verlag, New York. Kunin, (1983)
- [46] Leckie, F.A., Hayhurst, D.R., (1974), 'On Creep Rupture in Structures,' *Proceedings of Royal Society*, Vol. A340, p. 324.
- [47] Leckie, F.A., Hayhurst, D.R., (1977), 'Constitutive Equation for Creep Rupture,' *Acta Metallurgica*, Vol. 25, p. 1059.
- [48] MacKenzie, J.K., (1950), 'The Elastic Constants of a Solid Containing Spherical Holes,' *Proceedings Phys. Soc. B.*, Vol. 63, p. 2.
- [49] McLaughlin, R., (1977), 'A Study of the Differential Scheme for Composite Materials,' *International Journal of Engineering Science*, Vol. 15, p. 237.
- [50] Monkman, F.C., Grant, N.J., (1956), 'An Empirical Relation Between Rupture Life and Minimum Creep Rate,' *Proceeding of American Society for Testings of Materials*, Vol. 56, p. 593.

- [51] Mura, T., (1982), *Macromechanics of Defects in Solids*, Martinus Nijhoff, The Hague-Boston.
- [52] Murakami, S., (1983), 'Notions of Continuum Damage Mechanics and Its Application to Anisotropic Creep Damage Theory,' *ASME Journal of Engineering Materials and Technology*, Vol. 105, p. 99.
- [53] Needleman, A., Rice, J.R., (1980), 'Plastic Creep Flow Effects in the Diffuse Cavitation of Grain Boundaries,' *Acta Metallurgica*, Vol. 28, p. 1315.
- [54] Nemat-Nasser, S., Taya, M., (1981), 'On Effective Moduli of an Elastic Body Containing Periodically Distributed Voids,' *Quarterly Applied Mathematics*, Vol. 29, p. 43.
- [55] Nemat-Nasser, T., Iwakuma, T., Hejazi, M., (1982), 'On Composites with Periodic Structure,' *Mechanics of Materials*, Vol. 1, p. 239.
- [56] Nix, W.D., Gibeling, J.C., (1985), 'Mechanisms of Time-Dependent Flow and Fracture of Metals,' in *Flow and Fracture at Elevated Temperatures*, Philadelphia, p. 1.
- [57] Onat, E.T., (1982) 'Representation of Inelastic Behavior in the Presence of Anisotropy and of Finite Deformation,' in *Recent Advances in Creep and Fracture of Engineering Materials and Structures*, eds. B. Wilshire and D.R.J. Owen, Pineridge Press, Swansea, U.K., p. 231.



- [58] Onat, E.T., Leckie, F.A., (1984), 'A Continuum Description of Creep Damage,' T.A.M. Report No. 469, University of Illinois at Urbana-Champaign.
- [59] Parks, D.M., (1977), 'The Virtual Crack Extension Method for Nonlinear Material Behavior,' *Computer Methods in Applied Mechanics and Engineering*, Vol. 12., p. 234
- [60] Rabotnov, Yu N., (1960), 'The Theory of Creep and Its Applications,' *Plasticity* (Proceedings, Second Symposium on Naval Structural Mechanics, E.H. Lee and P.S. Symonds, eds.), Pergamon Press, p. 338.
- [61] Rice, J.R., (1968), 'Mathematical Analysis in the Mechanics of Fracture,' in *Fracture* (ed. H. Liebowitz), Vol II Academic Press, New York, p. 191.
- [62] Rice, J.R., (1970), 'On the Structure of the Stress-Strain Relations for Time-Dependent Plastic Deformation in Metals,' *ASME Journal of Applied Mechanics*, Vol. 37, p. 728.
- [63] Rice, J.R., (1981), 'Constraints on the Diffusive Cavitation of Grain Boundary Facets in Creeping Polycrystals,' *Acta Metallurgica*, Vol. 29, p. 675.
- [64] Riedel, H., (1984), 'A Continuum Damage Approach to Creep Crack Growth,' in *Fundamentals of Deformation and Fracture*, ed. K.J. Miller, Cambridge University Press, p. 291.

- [65] Rodin, G.J., Parks, D.M., (1986a), 'On Consistency Relations in Nonlinear Fracture Mechanics,' to be published in the Journal of Applied Mechanics.
- [66] Rodin, G.J., Parks, D.M., (1986b), 'Constitutive Models of a Power-Law Matrix Containing Aligned Penny-Shaped Cracks,' to be published in the Mechanics of Materials.
- [67] Roscoe, R., (1952), 'The Viscosity of Suspensions of Rigid Spheres,' British Journal of Applied Physics, Vol. 3, p. 267.
- [68] Sanchez-Palencia, E., (1980), '*Non-Homogeneous Media and Vibration Theory*,' Springer-Verlag, New York.
- [69] Servi, I., Grant, N.J., (1951), '*Creep and Stress Rupture Behavior of Aluminum as a Function of Purity*,' Transactions AIME, Vol. 191, p. 909.
- [70] Sneddon, I.N., (1964), 'The Distribution of Stress in the Neighbourhood of a Crack in an Elastic Solid,' Proceedings of the Royal Society, Vol. A187, p. 229.
- [71] Talbot, D.R.S., Willis, J.R., (1985), 'Variational Principles for Inhomogeneous Non-linear Media,' IMA Journal of Applied Mathematics, Vol. 35, p. 39
- [72] Trampczynsky, W.A., Hayhurst, D.R., Leckie, F.A., (1981), 'Creep Rupture of Copper and Aluminum under Non-Proportional Loading,' Journal of Mechanics and Physics of Solids, Vol. 29. p. 353.

- [73] Tvergaard, V., (1985), 'On the Creep Constrained Diffusive Cavitation of Grain Boundary Facets in Creeping Polycrystals,' *Acta Metallurgica*, p. 1977.
- [74] Vainberg, M.M., (1964), '*Variational Methods for the Study of Nonlinear Operators*,' Holden-Day, San-Francisco.
- [75] Willis, J.R., (1982), 'Elasticity Theory of Composites,' *Mechanics of Solids, The Rodney Hill 60th Anniversary Volume*, ed. H.G. Hopkins and M.J. Sewell, Pergamon Press, Oxford, p. 653.
- [76] Willis, J.R., (1985), 'Variational Estimates for the Overall Response of an Inhomogeneous Nonlinear Dielectric,' *Proceedings, IMA Workshop on Homogenization and Composites*, Minneapolis, October 1984.
- [77] Yang, M., Weertman, J.R., Roth, M., (1984), 'Use of Small Angle Neutron Scattering to Study Grain Boundary Cavitation,' *Proceedings of the Second International Conference on Creep and Fracture of Engineering Materials and Structures*, ed. Wilshire, B. and Owen, D.R.J., p. 149.

## Appendix A

### Differentiation of the Eigenvalues with Respect to a Tensor.

The spectral decomposition for a second rank symmetric tensor in three-dimensional Euclidean space is given by <sup>1</sup>

$$\mathbf{T} = \sum_{i=1}^3 \sigma_i \mathbf{e}_i \otimes \mathbf{e}_i. \quad (\text{A.1})$$

Scalars  $\sigma_i$  and vectors  $\mathbf{e}_i$  are the eigenvalues and the eigendirections, respectively, defined as solutions of equations

$$\mathbf{T}\mathbf{e}_i = \sigma_i \mathbf{e}_i, \quad |\mathbf{e}_i| = 1, \quad i = 1, 2, 3. \quad (\text{A.2})$$

Decomposition (1) is admissible if all three eigenvalues are distinct. In this case the eigendirections are uniquely determined from the system of equations (2).

The derivative of the eigenvalue with respect to the tensor is defined in a projector sense

---

<sup>1</sup>We attempt to give a self-contained presentation of the subject. This intention partially explains the absence of reference sources. Nevertheless, the first three chapters of the book Gurtin, M. E., (1981) 'An Introduction to Continuum Mechanics,' Academic Press, are of importance for avoiding notational ambiguities, at least. Recent work of Carlson, D. E., Hoger, A. (1984) 'The Derivative of a Tensor-Valued Function of a Tensor,' Institute for Mathematics and its Applications, IMA Preprint Series 101, gives comprehensive review on differentiation of the eigenvalues.

$$\frac{d\sigma_i}{dT} \cdot \mathbf{A} = \frac{d}{d\alpha} \sigma_i(\mathbf{T} + \alpha \mathbf{A})|_{\alpha=0}, \quad (\text{A.3})$$

where  $\mathbf{A}$  is an arbitrary tensor, which belongs to the same class as  $\mathbf{T}$ ; e.g. second rank symmetric in three dimensions. As a set of the trial projectors we adopt

$$\mathbf{A}^{(k)} = \frac{1}{2}(\mathbf{e}_i \otimes \mathbf{e}_j + \mathbf{e}_j \otimes \mathbf{e}_i); \quad k = \begin{cases} k = i & \text{if } i = j \\ k = 1 + i + j & \text{otherwise} \end{cases} \quad (\text{A.4})$$

It should be sufficient to have six independent tensors to find the six components of the derivative tensor. A particular advantage of the choice is the orthonormality

$$\mathbf{A}^{(p)} \cdot \mathbf{A}^{(q)} = \begin{cases} 1 & \text{if } p = q \\ 0 & \text{otherwise} \end{cases}, \quad p, q = 1, 2, \dots, 6. \quad (\text{A.5})$$

The first three trial tensors introduce trivial calculations into evaluations of definition (3). Namely,  $\sigma_1$  remains unaltered by the substitution of  $\mathbf{A}^{(2)}$  and  $\mathbf{A}^{(3)}$  into definition (3). The right-hand side of the definition is equal to unity, upon the substitution of tensor  $\mathbf{A}^{(1)}$ . A possible sequence of calculations for the rest of the group, say for  $\mathbf{A}^{(4)}$ , includes:

- Solve the characteristic equation for eigenvalues  $\lambda$  of tensor  $\mathbf{T} + \alpha \mathbf{A}^{(4)}$

$$(\sigma_3 - \lambda) \left\{ (\sigma_1 - \lambda)(\sigma_2 - \lambda) - \frac{\alpha^2}{4} \right\} = 0.$$

- Choose the root which in the limit of small value of  $\alpha$  gives  $\sigma_1$ . (This is where the presumption of distinct eigenvalues comes into play.)
- Find the derivative of the root with respect to  $\alpha$ . Obviously, we do not have to obtain explicit algebraic solution of the characteristic equation. It is sufficient

to find the root via perturbation technique, keeping only linear terms in  $\alpha$ . It turns out that to the first order  $\sigma_1$  and  $\lambda_1$  are equal, so that

$$\frac{d\lambda_1}{d\alpha}|_{\alpha=0} = 0.$$

An analogous situation takes place for  $k = 5, 6$ .

If we represent the derivative tensor as

$$\frac{d\sigma_1}{dT} = \sum_{k=1}^6 \beta^{(k)} \mathbf{A}^{(k)}, \quad (\text{A.6})$$

then the results just outlined, and the orthogonality lead directly to the answer:

$$\frac{d\sigma_1}{dT} = \mathbf{A}^{(1)} = \mathbf{e}_1 \otimes \mathbf{e}_1. \quad (\text{A.7})$$

The second derivative of  $\sigma_1$  can be indirectly defined via the the first derivative of the tensor  $\mathbf{A}^{(1)}$

$$\frac{d\mathbf{A}^{(1)}}{dT}[\mathbf{A}] = \frac{d}{d\alpha} \mathbf{A}^{(1)}(\mathbf{T} + \alpha \mathbf{A})|_{\alpha=0}. \quad (\text{A.8})$$

The course of calculations is analogous to evaluation of definition (3). Tensors  $\mathbf{T}$  and  $\mathbf{T} + \alpha \mathbf{A}^{(k)}$  ( $k = 1, 2, 3$ ) have identical eigendirections, therefore the right-hand side of (8) is zero. For  $\mathbf{A}^{(k)}$ ,  $k > 3$ , the eigenvalues remain unaltered to the first order, therefore we have to solve system of equations (2) for the new eigendirections. Tensors  $\mathbf{A}^{(4)}$ ,  $\mathbf{A}^{(5)}$  produce non-zero contributions

$$\frac{d}{d\alpha} \mathbf{A}^{(1)}(\mathbf{T} + \alpha \mathbf{A}^{(4)})|_{\alpha=0} = \frac{1}{\sigma_1 - \sigma_2} \mathbf{A}^{(4)},$$

$$\frac{d}{d\alpha} \mathbf{A}^{(1)}(\mathbf{T} + \alpha \mathbf{A}^{(5)})|_{\alpha=0} = \frac{1}{\sigma_1 - \sigma_3} \mathbf{A}^{(5)}.$$

The derivative, fourth rank tensor, can be represented by

$$\frac{d\mathbf{A}^{(1)}}{d\mathbf{T}} = \frac{1}{2} \sum_{p=1}^6 \sum_{q=p}^6 \gamma_{pq} (\mathbf{A}^{(p)} \otimes \mathbf{A}^{(q)} + \mathbf{A}^{(q)} \otimes \mathbf{A}^{(p)}). \quad (\text{A.9})$$

Relations (9) contain twenty one coefficients  $\gamma_{pq}$ , which is in obvious parallel to the number of elastic constants for linear elastic materials. The second derivative is

$$\frac{d^2\mathbf{A}^{(1)}}{d\mathbf{T}^2} = \frac{1}{\sigma_1 - \sigma_2} \mathbf{A}^{(4)} \otimes \mathbf{A}^{(4)} + \frac{1}{\sigma_1 - \sigma_3} \mathbf{A}^{(5)} \otimes \mathbf{A}^{(5)}. \quad (\text{A.10})$$

Now we would like to address situations with repeated eigenvalues. The difficulties here are twofold.

- The eigendirections are not uniquely determined from (2), therefore spectral decomposition (1) is not admissible.
- The eigenvalues  $\lambda$  are not smooth in  $\alpha$ , if they are *ordered*, and obviously can not be differentiated.

We need a constructive alternative to resolve the matter. For convenience, we associate  $\mathbf{T}$  with the stress tensor and number the eigenvalues in the descending order. Within context of the main document we choose the maximum principal tensile stress  $\sigma_1$  as the invariant which partially governs material response. Though this proposition has transparent physical reasoning, we have mentioned <sup>2</sup> that it

---

<sup>2</sup>See section 2.3

contains ambiguity. The ambiguity is directly related to the discontinuity of  $\sigma_1$ , when the principal stresses (eigenvalues) are equal. Of course, possible numerical implementations become exceedingly vulnerable. We are looking for a substitute which:

- Must be the invariant of the stress tensor.
- May be chosen arbitrary close to the maximum principal tensile stress.
- Must be sufficiently smooth.

We introduce a sequence

$$\sigma^{(p)} := \frac{1}{p} \ln \left\{ \frac{\exp(p\sigma_1) + \exp(p\sigma_2) + \exp(p\sigma_3)}{3} \right\}, \quad p = 0, 1, \dots, \infty. \quad (\text{A.11})$$

By definition,  $\sigma^{(p)}$  is the invariant. Let us show that in the limit of infinite  $p$ , the invariant is equal to the maximum principal tensile stress. Expression (11) can be rewritten in a form

$$\sigma^{(p)} = \sigma_1 + \frac{1}{p} \ln \left\{ \frac{1 + \exp(p\sigma_2 - p\sigma_1) + \exp(p\sigma_3 - p\sigma_1)}{3} \right\}.$$

The operand of the logarithm is bounded by unity ( $\sigma_1 = \sigma_2 = \sigma_3$ ) and by one third ( $\sigma_1 > \sigma_2, \sigma_1 > \sigma_3$ ). In both cases, if  $p$  tends to infinity, the limit of the second term of the right-hand side is zero, therefore

$$\lim_{p \rightarrow \infty} \sigma^{(p)} = \sigma_1. \quad (\text{A.12})$$



A choice of large and finite  $p$  allows to prescribe the maximum principal tensile stress with arbitrary accuracy. The differentiation of (11) is straightforward, if the principal stresses do not coalesce.

There are two cases of repeated eigenvalues to be considered.

$\sigma_1 = \sigma_2 > \sigma_3$ . Formally, the derivative can be written via

$$\frac{d\sigma^{(p)}}{dT} = \frac{\sum_{i=1}^3 \exp(p\sigma_i) \frac{d\sigma_i}{dT}}{\sum_{i=1}^3 \exp(p\sigma_i)}. \quad (\text{A.13})$$

The derivatives of  $\sigma_1$  and  $\sigma_2$  are not defined; nevertheless, it can be shown (see, for example, the review paper) that

$$\frac{d(\sigma_1 + \sigma_2)}{dT} = \mathbf{I} - \mathbf{e}_3 \otimes \mathbf{e}_3,$$

where  $\mathbf{I}$  is the second rank identity tensor. The above formula is sufficient for a complete evaluation of the right-hand side of expression (13), namely

$$\frac{d\sigma^{(p)}}{dT} = \frac{\exp(p\sigma_1)(\mathbf{I} - \mathbf{e}_3 \otimes \mathbf{e}_3) + \exp(p\sigma_3)\mathbf{e}_3 \otimes \mathbf{e}_3}{2\exp(p\sigma_1) + \exp(p\sigma_3)}. \quad (\text{A.14})$$

$\sigma_1 = \sigma_2 = \sigma_3$ . The underlying argument is similar to the argument of the previous case:

$$\frac{d(\sigma_1 + \sigma_2 + \sigma_3)}{dT} = \mathbf{I}.$$

The expression for the derivative becomes extremely simple:

$$\frac{d\sigma^{(p)}}{dT} = \frac{1}{3}\mathbf{I}. \quad (\text{A.15})$$

We conclude the appendix by mentioning that the case of  $p = 0$ , defined via

$$\sigma^{(0)} := \lim_{p \rightarrow 0} \frac{1}{p} \ln \left\{ \frac{\exp(p\sigma_1) + \exp(p\sigma_2) + \exp(p\sigma_3)}{3} \right\}. \quad (\text{A.16})$$

An application of l'Hospitale's rule gives us

$$\sigma^{(0)} = \frac{1}{3} \text{tr} \mathbf{T}, \quad (\text{A.17})$$

so that

$$\frac{d\sigma^{(0)}}{d\mathbf{T}} = \frac{1}{3} \mathbf{I}, \quad \frac{d^2\sigma^{(0)}}{d\mathbf{T}^2} = \mathcal{O}. \quad (\text{A.18})$$

In the above,  $\mathcal{O}$  is the fourth rank zero tensor.

END

12-86

DTIC